الاية

بسم الله الرحمن الرحيم

قال تعالى (لَقَدْأَرْسَلْنَا رُسُلَنَا بِالْبَيِّنَاتِ وَأَنْزَلْنَا مَعَهُمُ الْكِتَابَ وَالْمِيزَانَ لِيَقُومَ النَّاسُ بِالْقِسْطِ وَأَنْزَلْنَا الْحَدِيدَ فِيهِ بَأْسٌ شَدِيدٌ وَمَنَافِعُ لِلنَّاسِ وَلِيَعْلَمَ اللَّهُ مَنْ يَنْصُرُهُ وَرُسُلَهُ بِالْغَيْبِ إِنَّ اللَّهَ قَوِيٌّ عَزِيزٌ)

صدق الله العظيم

سورة الحديد، (الاية 25)

Dedication

This thesis is dedicated to:

My parents

My husband

My family

My friends

And all who support me during my research

Acknowledgment

First and foremost I thank Allah, for guiding and give me strength to bring forth to light this thesis. All thanks, respect and sincere gratitude and appreciation are directed to my supervisor Professor Nafie Abd Allattief Almuslet, who gave me the opportunity to do this research with his guidance and support until i became able to create this thesis. I would like to thank my college and members of physics department for their encouragement and support. Great thanks to all people working in Sudan University of science and technology, especially the staff of the institute of laser for their support. My thanks also are directed to Egyptian Petroleum Research Institute (EPRI)) for aiding me to do the practical part of this research. Deep thanks to my husband for the unlimited support. Deep gratitude to my mother for her prayers, continuous encouragement and unconditional support which help me to complete this work. Finally i would like to express my thanks to my relatives and friends for their support and to my students, who have never stopped inspiring me.

Abstract

In this work laser Raman Spectroscopy was used to identify the unstable compounds in five samples of iron oxides (hematite, magnetite, goethite, akaganeite and 2-line ferrihydrite). Firstly iron oxide samples were prepared using Fe $(N0_3)_3$ $9H_2O$ and KOH with different molar ratios through the chemical method in lab .These samples were irradiated using 5mW frequency doubled Nd-YAG laser with 532 nm at room temperature. Spectra database was used for the spectral analysis of the Raman shift of these five samples. The obtained results showed that the bands of unstable compounds are appeared clearly in the spectra of the samples. Characteristic bands of hematite were appeared in the spectra of magnetite, goethite, akaganeite and 2-line ferrihydrite compounds while bands of magnetite compounds were appeared in the spectra of hematite. The laser power causes the bands to broaden and to undergo a small shift to lower wavenumbers. Other materials were appeared in spectra of the five samples, like disulfide, alkyl disulfide, chlorolkanes and aliphatic fluoro. Raman spectroscopy proved to be suitable for the identification of unstable compounds in hematite, magnetite, goethite, akaganeite and ferrihydrite and could be used for other materials.

المستخلص

في هذا البحث استخدمت مطيافية رامان الليزرية لتوصيف المركبات غير المستقرة الناتجة لأوكسيدات الحديد عند التحفيز الضوئى لخمسة عينات هى (الهماتيت، المجناتيت، الغوزيد، الكانيد وفريهدريد) . اولا حضرت العينات معمليا باضافة نترات الحديد مع اكسيد البوتاسيوم بمعدلات ملارية مختلفة . تم تشعيع هذه العينات باستخدام ليزر التردد المضاعف للنيوديوم- ياق ذى الطول الموجى 532 نانو ميتر بقدرة قدرها 5 ملى واط فى درجة حرارة الغرفة. استخدمت قاعدة البينات الطيفية لتحليل أطياف للعينات الخمسة . أوضحت النتائج المتحصل عليها ان المركبات غير المستقرة ظهرت فى كل أطياف العينات . حيث ظهرت حزم الهماتيت فى عينة المجناتيت والغوزيد، كانيد وفريهدريد , بينما ظهرت حزم أطياف المجناتيت فى الهماتيت. تسببت قدرة الليزر فى أزدياد عرض الحزمة مع تغير بسيط فى العدد الموجى مع ظهور بعض المواد الاخرى فى العينات مثل السيلكا ، اليفاتية فلورين، ثُنائِيُّ سَلْفيدِ و سَلْفيدِ . برهنت تقنية رامان الطيفية انها طريقة مناسبة لمعرفة المركبات غير المستقرة الموجودة فى الهماتيت ، المجناتيت ، الغوزيد، كانيد وفريهدريد ويمكن اسخدامها ايضا فى معرفة المركبات فى المواد الاخرى.

List of Contents

List of Tables

List of Figures

Chapter One

Laser in Spectroscopy, an Overview

1.1: Introduction

Knowledge about the structure and properties of atoms and molecules is based on spectroscopic investigation (Demtröder, W., 2013). Until today, these investigations rely on the mutual support of theory and experiment. With the invention of the laser in the 1960's the field of optical spectroscopy virtually exploded. Equipped with a monochromatic, intense and often tunable light source branches such as nonlinear and high-resolution spectroscopy rapidly evolved (Schmidt, F., 2007). Ultra-fast pulsed lasers nowadays allow time-resolved spectroscopy on the attosecond time-scale and frequency combs using ultra-stable lasers locked to weak but narrow molecular lines serve as frequency standards. It became customary to distinguish between the term spectroscopy, which is associated with the study of spectra of atoms and molecules in general, and spectrometry, which refers to the use of spectroscopic information to assess atomic and molecular number densities, i.e. concentrations Most of the optical spectroscopic or spectrometric methods are based upon the principles of either absorption, emission, fluorescence, ionization or scattering. A variety of techniques is regularly applied to solid, liquid and gaseous samples, exploiting a manifold of physical phenomena such as saturation and polarization or the photo-acoustic- and Raman-effect. They utilize a substantial part of the electromagnetic spectrum, restricted only by the lack of suitable light sources or optical components in some wavelength regions as listed in table (1.1). A further step was taken in the 1980's, when laser spectroscopy emerged from the universities as an analytical discipline with important and increasingly commercial applications in chemistry, medicine, geology and biology (Schmidt, F., 2007).

Table1-1: Wavelength range used in different types of spectroscopy

Radiation Type	Range (Hz)	Type of Transitions
gamma rays	$10^{10} – 10^{8}$	Rearrangement of elementary particle in nuclear transitions
X-rays	$10^{8} – 10^{6}$	Transitions between energy levels of inner electrons of atoms and molecules
Ultraviolet, visible	10^{6}- 10^{4}	Transitions between energy levels of valence electrons of atoms and molecules
Raman -infrared	$10^{4} – 10^{2}$	Transitions between vibrational levels (change of configuration)
microwaves	10^{2} - 1	Transitions between rotational levels (change of orientation)
Electron spin resonance (ESR)	$1\text{-}10^{-2}$	Transitions between electron spin levels in magnetic field
Nuclear magnetic resonance (NMR)	$10^{-2} – 10^{-4}$	Transitions between nuclear spin levels in magnetic fields

1.2: The Study Objectives

The aim of this study is to use Raman spectroscopy to identify the constitutes of iron oxides, specially the unstable compounds, which are entered in irons industry.

1.3: The Thesis Structure

The layout of this thesis include usage of laser in spectroscopy, (chapter1), which discussed the absorption spectroscopy, emission spectroscopy and laser in absorption spectroscopy, laser in emission spectroscopy, laser in scattering spectroscopy. Chapter two discussed the basic principles of Raman spectroscopy, types of Raman spectroscopy, experimental techniques of Raman spectroscopy, applications of Raman spectroscopy and literature

review. Chapter three explains the experimental part which includes the experimental setup, samples preparation and experimental procedure. Chapter four presents the results, analysis, discussion, conclusions and recommendations.

1.4: Spectroscopy

Spectroscopy was originally the study of the interaction between radiation and matter as a function of wavelength (λ). In fact, historically, spectroscopy referred to the use of visible light dispersed according to its wavelength, e.g. by a prism. Later, the concept was expanded greatly to comprise any measurement of a quantity as function of either wavelength or frequency. Thus it also can refer to a response to an alternating field or varying frequency (v). A further extension of the scope of the definition added energy (E) as a variable, once the very close relationship (Ivković et al. 2016) :

$$\Delta E = h\nu \qquad (1.1)$$

Was realized where h is the Planck constant (6.626×10^{-34} J·s). There are two main types of spectroscopy:

(i) Atomic spectroscopy

The study of transitions, in absorption or emission spectroscopy, between electronic states of an atom, is atomic spectroscopy. It deals with the interaction of electromagnetic radiation with atoms which are most commonly in their lowest energy state (Solarz, R.W. and Paisner, J.A., 1986). Atomic spectra involve only transitions of electrons from one electronic energy level to another..There are three types of atomic spectroscopy:

- Atomic absorption spectroscopy (AAS).
- Atomic emission spectroscopy (AES).
- Atomic florescence spectroscopy

(ii) Molecular spectroscopy

When dealing with molecules, the interaction with light is primarily determined by the energy levels of the degrees of freedom 3n of the molecule.

These may be either associated with the movement of the electrons (electronic energy levels, possibly further differentiated by their spin), or of the atoms in the molecule (vibrational, rotational, or translational energy levels, i.e.motional energy states) (Le Ru, E. and Etchegoin, P., 2008).

1.4.1: Absorption Spectroscopy

Absorption spectroscopy refers to spectroscopic techniques that measure the absorption of radiation, as a function of frequency or wavelength, when electromagnetic radiation interacts with matter, energy is absorbed.

If the energy of incident photon corresponds to the energy gap between ground state and excited state of atoms or molecules the energy absorbed and atom or molecule excited where an electron promoted from it's to higher energy state. For example, in figure (1-1), E_1 and E_2 are the quantized energy levels and ΔE is the energy difference ($\Delta E = E_2 - E_1$) that must match the energy of the incident radiation (Le Ru, E. and Etchegoin, P., 2008).

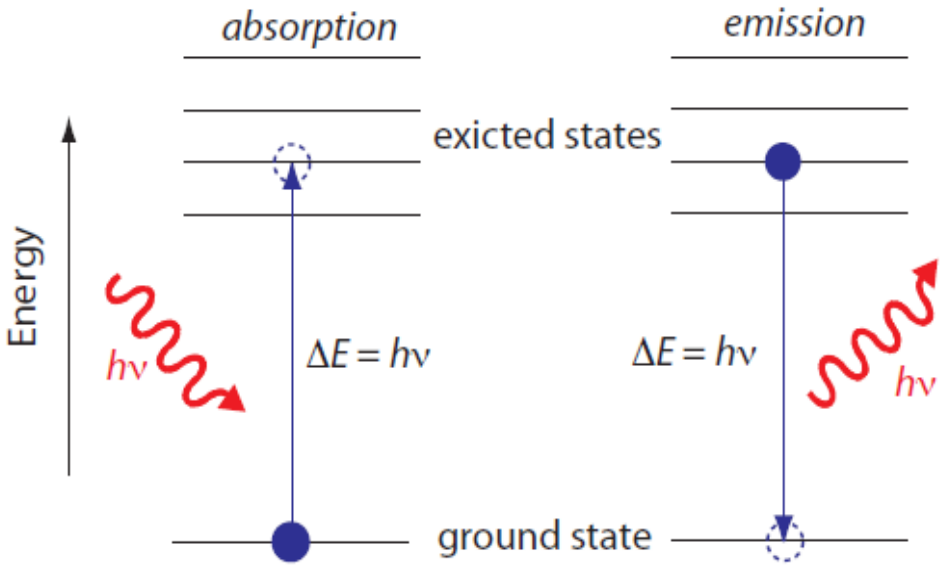

Figure (1.1): Absorption and emission energy process

Absorption spectroscopy is based on the Lambert-Beer law. This law may be understood as follows. As shown in fig. 1.2, let I_0 is the intensity incident

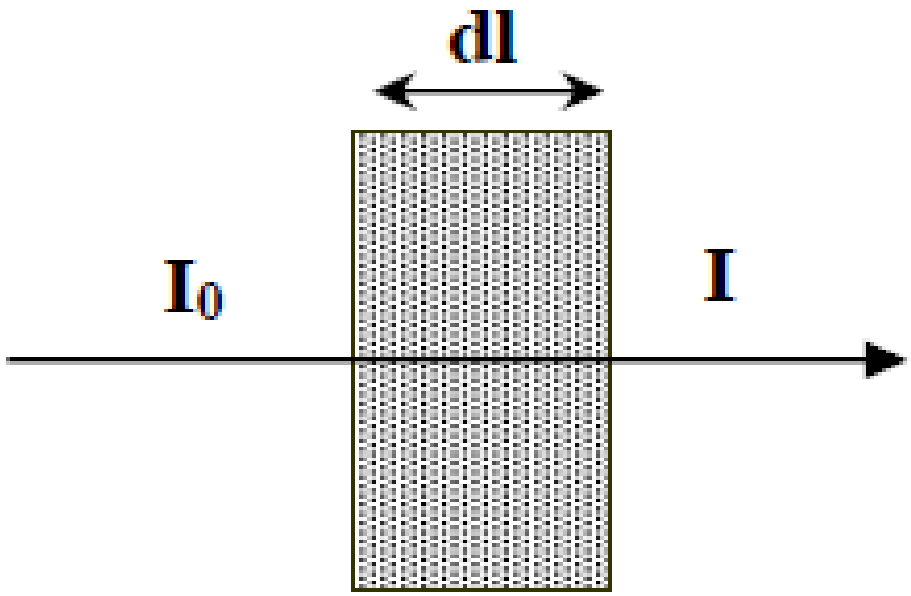

Figure (1.2): Schematic representation of light absorbed by sample of light incident

on the sample and I, is the intensity of the transmitted light. If the sample absorbs a part of light, then the law states that fraction of light (Log I_o/I) absorbed by the sample is proportional to the sample concentration (c) and the length of the sample dl so that,

$$\text{Log } I_o / I = \varepsilon \, c \, dI \qquad (1.2)$$

Where ε is the extinction coefficient (Tu, A.T., 1982). The probability per second that atom or molecule will absorb a photon, dP_{12}/dt, is proportional to the number of photons of energy hν per unit volume ρ(ν) and is usually expressed as:

$$\frac{d}{dt} \rho_{12} = B_{12} \rho(\nu) \qquad (1.3)$$

Where the constant B_{12} is the Einstein coefficient of induced absorption (units $J^{-1} m^3 s^{-2}$). It depends on the electronic structure of the atom, i.e. on its electronic wave functions in the two levels 1 and 2. Each absorbed photon of energy hν decreases the number of photons in one mode of the radiation field by one (Berman, P.R. and Malinovsky, V.S., 2010).

1.4.1.1: Atomic Absorption Spectroscopy

Is a technique for measuring quantities of chemical elements present in environmental samples by measuring the absorbed radiation by the chemical element of interest this is done by reading the spectra produced when the sample is excited by radiation. The atoms absorb the light energy of a specific wavelength and make transitions to higher energy levels (García, R. and Báez, A.P., 2012). As the number of atoms in the light path increases, the amount of light absorbed increases in a predictable way. By measuring the amount of light absorbed, a quantitative determination of the amount of analytic element present can be made. The use of special light sources and careful selection of wavelength allow the specific quantitative determination of individual elements in the presence of others. The atom cloud required for atomic absorption measurements is produced by supplying enough thermal energy to the sample to dissociate the chemical compounds into free atoms. Supplying a solution of the sample into a flame aligned in the light beam serves this purpose. Under the proper flame conditions, most of the atoms will remain in the ground state form and are capable of absorbing light at the analytical wavelength from a source lamp. The ease and speed at which precise and accurate determinations can be made with this technique have made atomic absorption one of the most popular methods for the determination of metals (Beaty, R.D. and Kerber, J.D., 1978).

Atomic absorption spectra consist of few dark lines. It is also of three types. They are:

1- Continuous absorption spectra**:** it consists of absence of continuous wavelength range. When an unexcited substance is placed between the source and prism then continuous absorption spectrum is produced. That is when a blue glass is placed between the source of white line and prism, then all wavelengths except blue are continuously absorbed.

2- Line absorption spectra: It consists of absence of sharp dark lines and is produced when an unexcited source of white light and prism that is, when a sodium vapour lamp is placed between the prism and tungsten filament, then two dark lines in yellow region corresponding to wavelengths 5890 A^0 and 5896 A^0 are appeared in line absorption spectra due to absorption in chromospheres.

3- Band absorption spectra: It consists of absence of sharp dark bands and is produced when unexcited substance in molecular state is placed between the source and prism (Taher, A.A.M., 2014).

1.4.1.2: Molecular Absorption Spectroscopy

A. Molecule can only absorb a particular frequency, if there exists within the molecule an energy transition of magnitude E = h ν**.** When molecular absorb energy and get transition to excited then either of the flowing energy change occur: Transitions on electron to high energy level.

B. Change in the intermolecular vibrations of molecule.

C. Transitions between electronic levels are found in the ultraviolet (190-400 nm) and visible (400-800 nm) energy regions.

D. Transitions between vibrational energy levels within the same electronic level are found in near infrared (14000–4000 cm^{-1}) and mid infrared (4,000 cm^{-1} to 400 cm^{-1}) regions.

E. Transitions between rotational energy levels are found in far infrared (500-20 cm^{-I}) and microwave regions.

F. Change of moment of inertia of the molecule around the center of gravity.

Electronic Transitions involve jumps to and from the different sublevels and resulting UV absorption spectra are observed in the form of a band because superposition of vibrational and rotational energies on electronic energy The absorption of X-rays result into transitions between inner shell electron of

atoms while only valence electron are involved in transitions when visible or ultraviolet radiation is absorbed. in case of lighter elements X-rays absorptions spectra independent of the element in free combined state. However, visible and ultraviolet spectra are effected by environment around the element (DR,H .Kaur, 2001).

1.4.2.: Emission Spectroscopy

The radiation field can also induce atoms or molecules in the excited state E_2 to make a transition to the lower state E_1 with simultaneous emission of a photon of energy hν. Figure (1.1). This process is called induced (or stimulated) emission. The induced photon of energy hν is emitted into the same mode that caused the emission. This means that the number of photons in this mode is increased by one. The probability dP_{21}/dt that one molecule emits one induced photon per second is in analogy to

$$\frac{d}{dt}\,\rho_{21} = B_{21}\,\rho(\nu) \qquad (1.4)$$

The constant factor B_{21} is the Einstein coefficient of induced emission. An excited molecule in the state E_2 may also spontaneously convert its excitation energy into an emitted photon hν. This spontaneous radiation can be emitted in the arbitrary direction k and increases the number of photons in the mode with frequency ν and wave vector k by one. In the case of isotropic emission, the probability of gaining a spontaneous photon is equal for all modes with the same frequency ν but different directions k. The probability per second $dP^{Spon}{}_{21}/dt$ that a photon $h\nu = E_2 - E_1$ is spontaneously emitted by a molecule, depends on the structure of the molecule and the selected transition 2 to 1, but it is independent of the external radiation field (Demtröder, W., 2008). For atoms excited by a high-temperature energy source this light emission is commonly called atomic or optical emission (atomic-emission spectroscopy) and for atoms excited with light it is called atomic fluorescence (atomic-fluorescence spectroscopy). For molecules is called Photoluminescence (Taher, A.A.M., 2014).

1.4.2.1: Photoluminescence

The transitions within the molecules are usually studied by the selective absorptions of radiation passing through them and less commonly by emission processes such as fluorescence and phosphorescence (Stuart, B.H., 2004).

In organic molecule whose ground state is a singlet, there are several energetically accessible triplet excited states (two unpaired spins). Following excitation into the manifold of singlet excited states by absorption. Molecule may undergo non radioactive decay (inter system crossing) to the manifold of triplet states the triplet state may emit a photon as the molecule decays back to the ground state (phosphorescence) (Taher, A.A.M., 2014).

1.4.2.2: Chemiluminescence

Chemiluminescence occurs when a chemical reaction produces an electronically excited species which emits a photon in order to reach the ground state. These sorts of reactions can be encountered in biological systems; the effect is then known as bioluminescence. The number of chemical reactions which produce chemiluminescence is small. However, some of the compounds which do react to produce this phenomenon are environmentally significant (Lin, J.M. and Yamada, M., 2003)

1.4.2.3: Atomic Emission Spectroscopy

In atomic emission, a sample is subjected to a high energy, in order to produce excited state atoms, capable of emitting light. The energy source can be an electrical arc, a flame, or more recently, plasma. The emission spectrum of an element exposed to such an energy source consists of a collection of the allowable emission wavelengths, commonly called emission lines, because of the discrete nature of the emitted wavelengths. This emission spectrum can be used as a unique characteristic for qualitative identification of the element. Atomic emission using electrical arcs has been widely used in qualitative analysis. Emission techniques can also be used to determine how much of an element is present in a sample. For a "quantitative" analysis, the intensity of

light emitted at the wavelength of the element to be determined is measured. The emission intensity at this wavelength will be greater as the number of atoms of the analyte element increases. The technique of flame photometry is an application of atomic emission for quantitative analysis (Boss, C.B. and Fredeen, K.J., 1999.).

1.4.2.4: Atomic-Fluorescence Spectroscopy

This technique incorporates aspects of both atomic absorption and atomic emission. Like atomic absorption, ground state atoms created in a flame are excited by focusing a beam of light into the atomic vapor. Instead of looking at the amount of light absorbed in the process, however, the emission resulting from the decay of the atoms excited by the source light is measured. The intensity of this ‘‘fluorescence’’ increases with increasing atom concentration, providing the basis for quantitative determination. The source lamp for atomic fluorescence is mounted at an angle to the rest of the optical system, so that the light detector sees only the fluorescence in the flame and not the light from the lamp itself. It is advantageous to maximize lamp intensity with atomic fluorescence since sensitivity is directly related to the number of excited atoms which is a function of the intensity of the exciting radiation. (Beaty, R.D. and Kerber, J.D., 1978). The main types of atomic fluorescence are (a) resonance fluorescence, (b) direct line fluorescence and (c) stepwise line fluorescence. Resonance fluorescence occurs when atoms absorb and re-emit radiation of the same wavelength; this is the predominant form of fluorescence measured by analytic chemists. These wavelengths can be different. Direct line fluorescence is quenched when an atom is excited from the ground state to a higher excited electronic state and then undergoes a direct radiational transition to a metastable level above the ground state. Stepwise line fluorescence occurs when the upper energy levels of the exciting and the fluorescence line are different. The excited atoms may

undergo deactivation, usually by collisions to a lower excited state rather than return directly to ground state (Sanchez-Rodas et al .2010).

1.5: Laser in Spectroscopy

The advent of stable lasers in late 1960's as an exciting source and completely replaced the mercury lamp has become usefulness of variety spectroscopy due to many characteristics (Bumbrah, G.S. and Sharma, R.M., 2016):

1-There is the large spectral density of power attainable from most types of lasers, such as Argon ion laser (488 and 514.5 nm), Krypton ion laser (530.9 and 647.1 nm), Helium–Neon (He–Ne) (632.8 nm), Near Infrared (IR) diode lasers (785 and 830 nm), Neodymium–Yttrium Aluminum Garnet (Nd:YAG) and Neodymium–Yttrium Ortho-Vanadat (Nd: YOV) (1064 nm) which can exceed that from incoherent light sources by several orders of magnitude. This feature has many consequences. On one hand, noise problems (either coming from background radiation or due to the detector) can be significantly reduced, which implies an improvement of the signal-to-noise ratio. On the other hand, the high intensity of the radiation provided by lasers allows the study of nonlinear phenomena, such as multi photon processes or saturation phenomena, which otherwise were not easily accessible by conventional linear spectroscopy (Solé et al .2005).

2- The small divergence of the radiation beam. This makes the handling and control of the light beam much easier and allows its confinement in integrated optics devices. From the viewpoint of spectroscopy, some examples of the advantage of a small divergence in collimated laser beams can be mentioned: measurements of very small absorption coefficients, which can be achieved by using long path lengths through the sample (even by using wave-guided configuration); and the efficient collection and imaging onto the detection system of the incoming radiation from a very small interaction zone of the sample. This can be particularly useful, for instance, in Raman scattering or low-level fluorescence spectroscopy (Solé et al .2005).

3-The narrow spectral width that can be obtained with some type of lasers constitutes an advantage that has a particular impact on the development and application of high-resolution spectroscopy techniques. In fact, the spectral resolution provided by some lasers may exceed that of the largest monochromators by several orders of magnitude.

4-The possibility of continuously tuning the wavelength, with ball of the aforementioned characteristics. Actually, the use of lasers in spectroscopy can turn out to be less expensive than it might seen, since a tunable laser could replace an intense source of radiation and a high-resolution, high-priced monochromators (Solé et al .2005).

5-The possibility of pulsed lasers supplying intense short and ultra-short pulses up to the fmtosecond range. This has permitted the study of fast and ultra fast, such as various fast relaxation processes in solids (Solé et al .2005).

6-With laser beams, we can deal with the phenomena that occur when many mutually coherent waves are superimposed. Many experiments in laser spectroscopy depend on the coherence properties of the radiation. From the viewpoint of spectroscopy, the use of coherent light beams can be applied to measurements that require a high resolving power (Solé et al .2005).

Due to this factor a variety of configurations and methods for laser spectroscopy have been developed. These methods are extensively used for quantitative and qualitative analysis of atoms, ions, and chemical species. We will consider a few selected types of laser in absorption spectroscopy, laser in emission spectroscopy and laser in scattering spectroscopy as examples (Nafie A. Almuslet., 2009).

1.5.1: Laser in Absorption Spectroscopy (LAS)

Laser-based absorption spectroscopy (lAS) is a powerful technique for qualitative and quantitative studies of atoms and molecules in gas phase. An important field of use of LAS is the detection of species in trace gas concentrations, which has applications not only in physics and chemistry but

also in biology and medicine, encompassing environmental monitoring, regulation of industrial processes and breath analysis. Although a large number of molecular species can successfully be detected with established LAS techniques. When the laser light passes through a cavity which is filled by a gas sample for investigation (Schmidt, F., 2007).The attenuation of the light passing a sample originates from the destructive interference between the incident field and the coherently driven dipole moments of the atoms/molecules. In a simple, phenomenological picture one can consider the electromagnetic radiation as being composed of photons, and each atom or molecule having a unique set of states with distinct energies. Exposed to narrowband light, an atom or molecule might absorb a photon if its frequency ν (or wavelength λ) is such that its energy corresponds to the energy difference between the two states i and j, according to $h\nu = E_i - E_j$. The presence of a particular constituent in a gas can then be determined by probing the gas with light whose frequency corresponds to only that of a transition of the atom or molecule. The amount of absorbed light can be related to the concentration of the analyte if calibration measurements with samples with known concentrations under otherwise identical conditions have been performed or by using a model of the absorption process. According to Beer's law, the attenuation of power of the light p(v) that passes through a uniform gaseous sample with a number density of absorbers n (cm^{-3}) and the path length l (cm) is usually described by:

$$P(v) = P_0 \exp[-\sigma(v)nl] = P_0 \exp[-\alpha(v)] \qquad (1.5)$$

Where P_0 (v) denotes the power of the light prior to entering the medium and σ (v) (cm^2) refers to the absorption cross-section of the atomic or molecular transition (Schmidt, F., 2007). The dimensionless exponent in Beer's law, α (v), is often called absorption coefficient

For small absorption α (v) <<1, we can use the approximation, $e^{-\alpha} \approx 1$, and

(1.5) can be written:

$$P(v) = P_0 (1-\alpha (v)) \qquad (1.6)$$

$$\alpha (v)= P_0- P(v)/ P_0=\Delta P(v)/P0 \qquad (1.7)$$

The absorption coefficient $\alpha_{ij}(v)$ of the transition i → j with an absorption cross section σ_{ij} is determined by the density N_i of absorbing molecules (Schmidt, F., 2007) .

$$\alpha_{ij}(v) = [N_i – (g_i / g_j) N_j] \sigma_{ij} (v)=\Delta N \alpha_{ij}(v) \qquad (1.8)$$

In laser absorption spectroscopy, because of monochromaticity of laser light, the laser itself acts as monochromator. The directionality of laser beam allows propagating the beam along the absorption cell, which increases the signal-to noise ratio and consequently increasing the sensitivity. This also allows us to perform absorption measurements at low pressure. Finally, because of the high intensity of lasers, detector noise plays a minimal role in the absorption measurement. The sensitivity of the laser technique is often many orders of magnitude higher than that for conventional absorption spectroscopy (Nafie A. Almuslet., 2009).

1.5.1.1: Laser Photoacoustic Spectroscopy

Is another method of laser-absorption spectroscopy, beside direct transmission measurement, based on photoacoustic spectroscopy (PAS) measurements. In this method the wavelength dependence of the magnitude of acoustic signal changes, resulting from sample heating after laser absorption is recorded (Nafie A. Almuslet., 2009). The photoacoustic effect consists in the generation of sound when a material is illuminated with pulsed light. The PA effect can be divided in three steps: Heat release in the sample material due to relaxation of optical light absorption through molecular collisions, Acoustic and thermal wave generation due to localized transient heating and expansion, Detection of the acoustic signal in the PA cell using a microphone. In the first step, photons are absorbed by the material and internal energy levels are excited. In the second step, sound and thermal wave generation is

theoretically described by fluid dynamics and thermodynamics. The last step consists in the detection of the generated acoustic wave using a microphone (Besson, J.P., 2006).

1.5.2: Laser in Emission Spectroscopy

Lasers are used to produce different types of emission in atoms, ions and molecules. The monochromaticity, high intensity and directionality provide unique advantages for lasers in emission spectroscopy compared with conventional light sources (Nafie A. Almuslet., 2009).

1.5.2.1: Laser-Induced Breakdown Spectroscopy (LIBS)

Laser-induced breakdown spectroscopy (LIBS) is an atomic emission spectroscopy. Atoms are excited from the lower energy level to high energy level (Cremers, D.A. and Knight, A.K., 2006).The conventional excitation energy source can be a hot flame, light or high temperature plasma. The excited energy that holds the atom at the higher energy level will be released and the atom returns to its ground state eventually. The released energy is well defined for the specific excited atom, and this characteristic process utilizes emission spectroscopy for the analytical method. LIBS employ the laser pulse to atomize the sample and leads to atomic emission. Compared to the conventional flame emission spectroscopy, LIBS atomizes only the small portion of the sample by the focused laser pulse on a target surface, the target surface will get vaporized and a plasma is formed at the surface The bright plasma emission was viewed through a side window at right angles to the plasma expansion direction which makes a tiny spark on the sample. Because of the short-life of the spark emission, capturing the instant light is a major skill to collect sufficient intensity of the emitting species. Three major parts of the LIBS system are a pulse laser, sample, and spectrometer. Control system is usually needed to manage timing and the spectrum capturing. Figure (1.3) illustrates those three major components and a computer in the conventional LIBS (Cremers, D.A. and Knight, A.K., 2006).

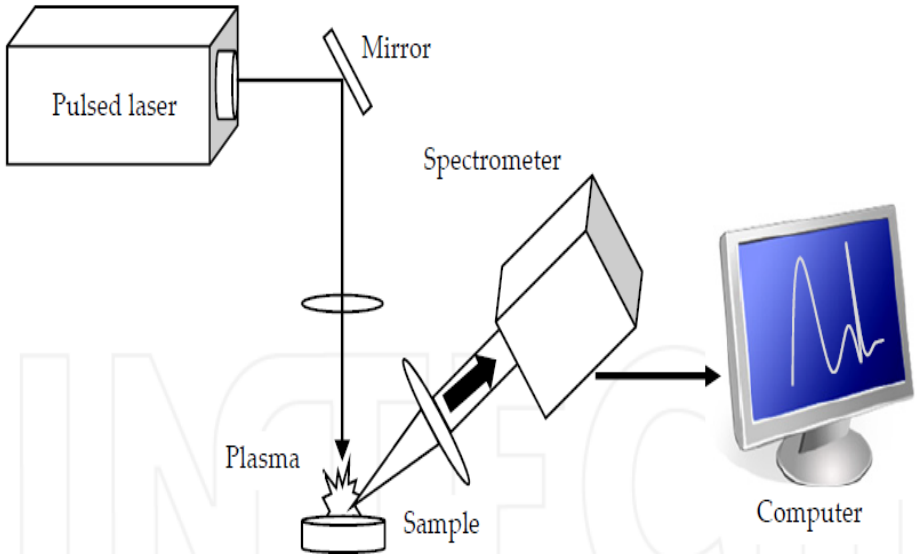

Figure (1.3): schematic representation for laser induced breakdown spectroscopy illustrating the principal components

1.5.2.2: Laser-Induced Fluorescence

Laser induced florescence is a versatile technique in which atomic or molecular species are irradiated with laser radiation in specific wavelength range usually in ultraviolent and visible spectral region for electronic spectroscopy that in resonance with the differences in molecular energy levels, such resonantly tuned radiation has fairly good probability of including a transition to the excited state of molecules, which may be followed by relaxation of molecules to the ground electronic state by spontaneous emission of photon whose energy corresponds to the separation in molecular energy levels (Lin, J.M. and Yamada, M., 2003). LIF spectroscopy is a sensitive and powerful technique for detecting molecules and atoms, measuring species concentration and energy level Population distributions, and for probing energy transfer processes in molecules and atoms. The measurement is based on the natural fluorescence of molecules and atoms, the fluorescence signal is detected using a photomultiplier or other light sensitive detector. The intensity of fluorescence signal is proportional to the number of

excited species. The most successful areas of LIF are in combustion diagnostics, in magnetically confined plasmas, in analytical chemistry, medicine and biochemistry to study the structure, reaction mechanisms and to measure species concentrations in oil industry and environmental studies (Nafie A. Almuslet., 2009).

1.5.3: : Laser in Scattering Spectroscopy

When a laser light is passed through a transparent substance, a small amount of the radiation energy is scattered (Kumar et al. 2013). Light scattering consists out of two scattering types; elastic scattering, the most intense form of scattering, which is known as Rayleigh scattering, and inelastic scattering, which occurs as a result of energy exchange between the molecules and incident photon. The last event is a very weak event, which involves only one in 10^6–10^8 of the scattered photons (Hassanein, R., 2011).

1.5.3.1: Raman Spectroscopy

Raman spectroscopy is a spectroscopic technique used in condensed matter physics and chemistry to study vibrational, rotational and other low-frequency modes in a system. It is based on an inelastic scattering process, or Raman effect of monochromatic light, usually from a laser in the visible, near-infrared or near-ultraviolet range of electromagnetic spectra (Sur, U.K., 2013). The history of Raman spectroscopy thus dates back to 1928 but the technique did not generalize until the 70s, with the development of lasers technology. In the Raman effect, photons of the exciting radiation interact with molecules of the sample being irradiated. The energies of the scattered photons are either increased or decreased relative to the exciting photons by quantized increments which correspond to the energy differences in the vibrational and rotational energy levels of the molecule. These scattered lines, called Raman lines, are characteristic of the vibrational or rotational modes of the substance and are therefore a "fingerprint" of that substance (Kumar et al.

2013). Figure (1.4) shows the energy levels of Raman scattering and infrared absorption.

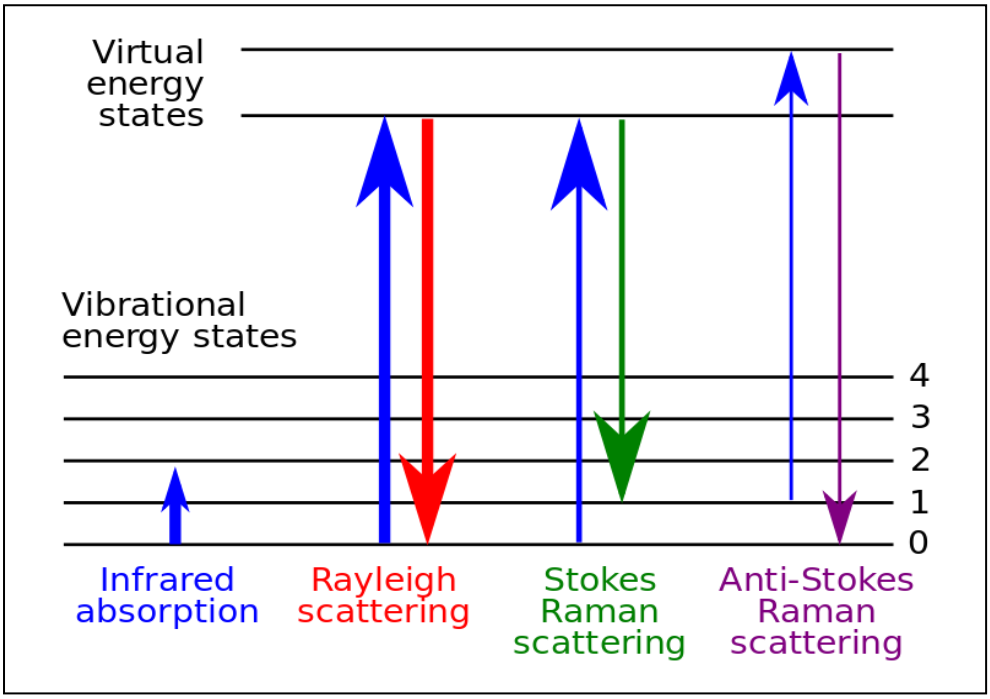

Figure (1.4): Diagram showing Raman scattering, Rayleigh scattering and infrared absorption

When the energy of the incident radiation is not large enough to excite the molecule from the ground state to the higher electronic state, the molecule will be excited to a virtual state between the ground state and higher electronic state (Sur, U.K., 2013). In the case of Rayleigh scattering, the wavelength of the scattered photon is same as the incident photon. In the case of Stokes scattering, the photon is scattered at a lower energy. In anti-Stokes scattering, the initial state is the excited state and the scattered photon has higher energy than the incident one. At room temperature, the molecule is principally in its ground vibrational state. A small number of molecules will be in a higher vibrational level and as a result, the photon is scattered at higher energy (shifted wavelength towards the blue). Thus, anti-Stokes scattering is much weaker compared to Stokes scattering. In Raman spectroscopy, the sample is illuminated with a laser beam. Wavelengths close to the laser line (due to the Rayleigh scattering) are filtered out and the rest of

the unfiltered light is dispersed onto a detector. As the Raman scattering is very weak compared to the Rayleigh scattering, the separation of Raman signals is necessary. Historically, Raman spectrometers used holographic diffraction gratings to achieve a high degree of incident rejection. However, modern instrumentation universally employs notch filters for incident beam rejection. Introduction of fast-Fourier transform (FFT) based spectrometers, confocal microscopes and charge coupled device (CCD) detectors has brought a new dimension in Raman instruments, providing very high sensitivity. Raman spectroscopy can be further applied for microscopic analysis of materials, such as polymers, ceramics and biological cells. Now in modern Raman instruments, several laser wavelengths may be employed to obtain the best detection limit of the Raman signal with sensitivity for the Raman analysis (Hassanein, R., 2011).

Chapter Two

Raman Spectroscopy Basic Principles and Applications

2.1: Introduction

This chapter exposed the theoretical background of Raman spectroscopy**,** depolarization ratio (Pp) measurement, the experimental techniques with different types of excitation sources, sample illumination, sample Preparation and handling, types of Raman instruments, operational parameters, advantages and disadvantages of Raman spectroscopy, types of Raman spectroscopy and its applications, and literature review

2.2: Basic Principles of Raman Spectroscopy

The Raman spectroscopy occurs when monochromatic light impinges upon a molecule and interacts with the bonds of this molecule. For the spontaneous Raman effect to take place, the molecule is excited by a photon from the ground state to a virtual energy state (Joshi et al . 2008).The molecule can relax and return to the ground state by emission of a photon whose energy is the same as that of the exciting radiation resulting in elastic Rayleigh scattering. But a very small part (approximately 10^{-7} photons) of the scattered light can also have frequencies that are smaller than those of the elastically scattered part because a part of the energy of the incoming photons was employed to excite molecules to a higher vibrational state. As a result, the emitted photons will be shifted to lower energy, i.e., light with a lower frequency. This shift is designated the Stokes shift and it is a fingerprint of the molecules. The difference in energy between the original state and the final state corresponds to a vibrational mode far from the excitation wavelength. If the process starts from a vibrationally excited state v = 1 and relaxes to the ground state v = 0, then the emitted photons will be shifted to higher frequency which is designated the Anti-Stokes shift. Compared with the Stokes-shifted light, the Anti-Stokes shifted radiation has a lower intensity because of the small population of the vibrationally excited state compared to

that of the ground state of the molecule at room temperatures (Reichenbächer, M. and Popp, J., 2012).

2.2.1: Classical Theory

For predicting whether a molecular vibration is Raman active or not, the classical theory is introduced. Raman scattering phenomena may be described using a classical explanation in terms of the electromagnetic radiation by multiples induced by the electric field of the incident radiation. For example, if a diatomic molecule is irradiated by an incident light (w_0), an electric dipole moment (P) is induced (Ding, J., 2010). The size of the dipole moment induced by a field of magnitude E is given by the polarizability (α) of the molecule

$$P = \alpha E \qquad (2.1)$$

Light consists of oscillating electric and magnetic fields. For light of frequency w_0, the magnitude of the electric field may be written:

$$E = E_0 \cos 2\pi w_0 t \qquad (2.2)$$

Thus, the induced dipole moment oscillates in phase with the applied field:

$$P = \alpha E_0 \cos 2\pi w_0 t \qquad (2.3)$$

The polarizability will depend upon the geometry of the molecule; as the molecule vibrates, the polarizability will change. If we write the polarizability as a Taylor series expansion in a nuclear coordinate r about its equilibrium position (r_0), then:

$$\alpha = \alpha_0 + (d\alpha/dq)_0 (r - r_0) + \ldots\ldots \qquad (2.4)$$

Alternatively, we can expand α in terms of q, the vibrational displacement coordinate of the i the normal mode. The classical normal mode vibration is

$$q = q_0 \cos 2\pi w_i t \qquad (2.5)$$

Where w_i is the frequency of normal mode i. In this classical picture, we then find that:

$$P = \alpha_0 E_0 \cos 2\pi w_0 t + \tfrac{1}{2}(d\alpha/dq) q_0 E_0 \cos 2\pi [(w_0 + w_i) t + (w_0 - w_i) t] \qquad (2.6)$$

Equation (2.6)) reveals that the induced dipole moment is created at three

distinct frequencies, namely w_0, (w_0 + w_i), and (w_0 - w_i), which results in scattered radiation at these same three frequencies. The first scattered frequency is responsible for Rayleigh scattering at v_0 while the second and third terms describe inelastic Raman scattering shifted by the frequency of the vibration, w_0, to frequencies which are higher (anti-Stokes,w_0-w_i) and lower (Stokes,w_0 +w_i), respectively, than the incident light frequency. In addition, equation (2.6) shows that for Raman scattering to occur the conduction is:

$$d\alpha /dq \neq 0 \qquad (2.7)$$

That is, the polarisability of the molecule must change during a vibration if that vibration is to be Raman active. If the polarizability does not change during a vibration, this coefficient is zero, and the vibration is not Raman-active (Gardiner, D.J., 1989). For pure rotational Raman, the polarizability changes because during molecular rotation the orientation of the molecule with respect to the electric field E of incident light changes. For a diatomic molecule if the rotational frequency is w_R the time dependent polarizability is given by: $Q=Q_0 \cos 2\pi (2w_R t)$. In this case the factor $2w_R$ arises because during a complete rotation (by 2π) the molecule assumes same orientation twice (for rotation by π and 2π). Then in analogy to equation (2.6) for rotational Raman one can write that:

$$P=\alpha_0 E_0 \cos (2\pi w_0 t) + \tfrac{1}{2} (d\alpha/dq_0) E_0 \cos 2\pi [(w_0+ 2w_R)t+ (w_0- 2w_R)t] \qquad (2.8)$$

According to this equation the frequencies of Stokes and anti-Stokes lines are w_0 - $2w_R$ and w_0 + $2w_R$, respectively (Kiefer, J., 2015).

Thus very simple classical consideration can explain the appearance of both vibrational and rotational change of stoke and anti stoke line. However once, intensity of stoke and anti stoke line is considered, this classical theory is most unsatisfactory, since it predict that stoke and anti stoke line should be of equal intensity, where as in the practice of vibrational change the latter are very much less intense than former. A quantum mechanical approach

however predicts that anti stoke line will be much weaker than stoke line for vibrational transitions (Straughan, B. ed., 2012).

2.2.2: Quantum Theory

Consider a vibrating molecule and suppose that it is represented by a harmonic oscillator. The vibrational energy E_{vib} of the ground state of this molecule is (Gustafsson, U., 1993):

$$E_{vib}=(n+ ½) hw_{vib} \qquad (2.9)$$

Where h is Plank's constant, w_{vib} is the vibrational ground frequency, and n is the vibrational quantum number controlling the energy of that particular vibration and it has values of 0, 1, 2, 3, etc. The vibrational energy levels in the ground state are thus equally spaced, quantified, by the amount w_{vib}. In the quantum mechanical model, light scattering is depicted as a two-photon process. The first step is the interaction between a photon of frequency w and a molecule which raise the molecule to a higher energy state. The second step involves the release of another photon and the relaxation of the molecule. Rayleigh scattering arises from transitions which start and finish at the same vibrational energy level. Stokes Raman scattering arises from transitions which start at the ground state vibrational energy level and finish at a higher vibrational energy level, w- $w_{vib,}$ whereas anti-Stokes Raman scattering involves a transition from a higher to a lower vibrational energy level w + w_{vib}. At normal room temperatures, most molecular vibrations are in ·the ground, n = 0 state and thus the anti-Stokes transitions are less likely to occur than the Stokes transitions resulting in the Stokes Raman scattering being more intense. This greater relative intensity becomes increasingly greater as the energy of the vibrations increases and the higher vibrational energy levels become less populated at any given temperature. For this reason it is usually the Stokes Raman scattering which is routinely studied and implied in Raman spectroscopy (Gustafsson, U., 1993). This intensity effect can clearly be seen

in figure (2.1), where the complete Stokes and anti-Stokes Raman spectrum of carbon tetrachloride is shown.

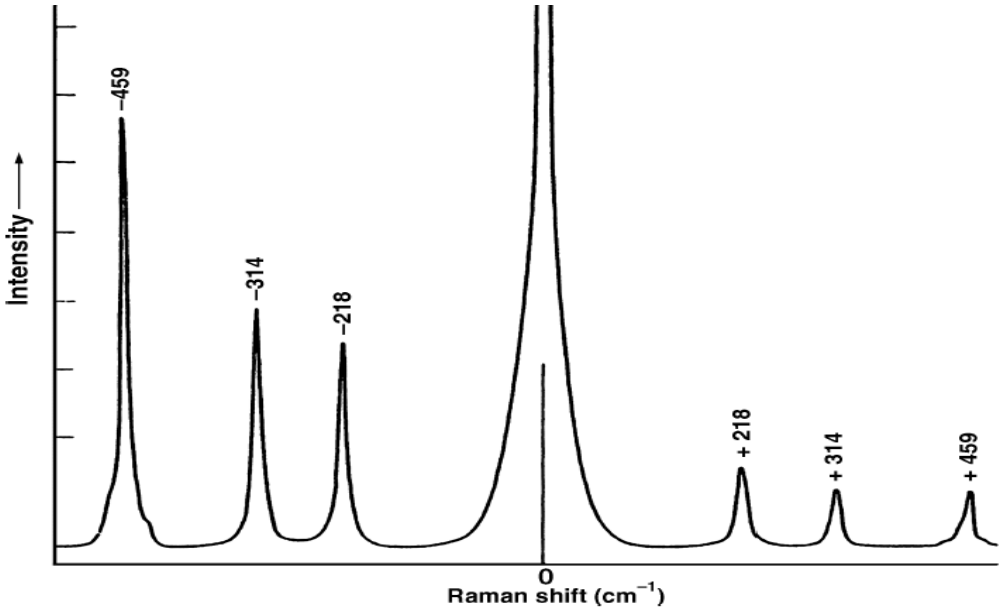

Figure (2.1): Stokes and anti-Stokes Raman spectrum of carbon tetrachloride

2.3: Depolarization Ratio (Pp) Measurement

The ratio of the spectral band intensities measured along two axes is called the depolarization ratio. By convention, the ratio is the perpendicular polarized intensity divided by the parallel intensity. For laser light polarized along the *y* axis as in figure (2.2), the equation for depolarization ratio is as follows:

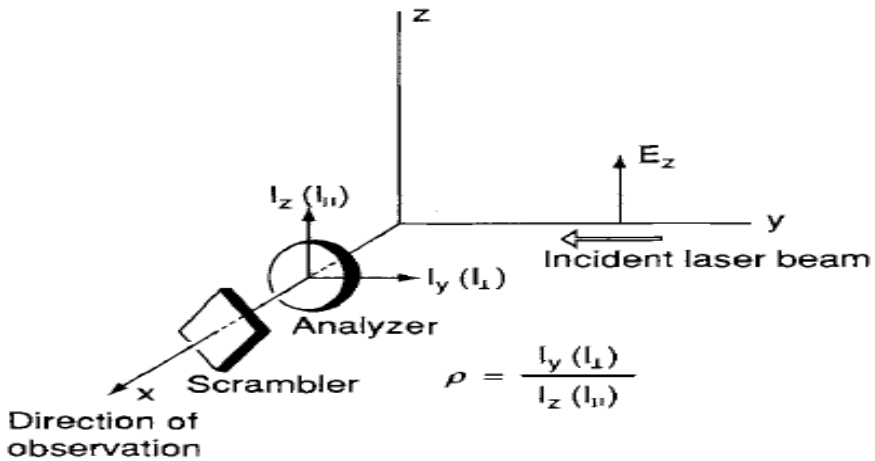

Figure (2.2):90° scattering geometry

$$Pp = I_y/I_z = 3\gamma^2/ (45\ \alpha\text{-}^2+4\gamma^2) \qquad (2.10)$$

Where $\alpha\text{-}^2$ and γ^2 are define the derivative of the polarisability tensor

($\alpha = \bar{\alpha} + \gamma$) that can be written as (Gilson, T.R. and Hendra, P.J., 1970):

$$\bar{\alpha} = \frac{1}{3}(\alpha_{xx} + \alpha_{yy} + \alpha_{zz}) \qquad (2.11)$$

$$\gamma^2 = \frac{1}{2}(\alpha_{xx} - \alpha_{yy})^2 + (\alpha_{yy} - \alpha_{zz})^2 + (\alpha_{zz} - \alpha_{xx})^2 + 6(\alpha_{xy}^2 + \alpha_{yz}^2 + \alpha_{xz}^2) \qquad (2.12)$$

Measuring the depolarization ratio for a Raman band yields information about the values of $\bar{\alpha}$ and γ. From this, we can deduce symmetry information for the vibration causing the Raman band. For example, a vibration mode which is not totally symmetric produces values of $\bar{\alpha} = 0$ and $\gamma \neq 0$. This gives a depolarization ratio value of ¾. For modes which are totally symmetric, the value of $\gamma = 0$ and the value of the ratio = 0. Other modes have symmetry yielding non-zero values of ($\bar{\alpha} \neq 0$). This leads to depolarization ratios between the values of zero and ¾. (Lin-Vien et al .1991, Ferraro, J.R., 2003).

2.4: Types of Raman Spectroscopy

2.4.1: Resonance Raman Spectroscopy

Many substances, especially colored ones, may absorb laser beam energy and create strong fluorescence which contaminates Raman spectrum. This is one of the central problems in Raman spectroscopy especially when UV lasers are used. However, it was found that under certain conditions some types of colored molecules can produce strong Raman scattering instead of fluorescence. This effect was called Resonance Raman (Hassanein, R., 2011). Resonance Raman (RR) scattering that occurs when the sample is irradiated with an exciting line whose energy corresponds to that of the electronic transition of a particular chromophoric group in a molecule (responsible for the molecule's coloration). Under these conditions the intensities of Raman bands originating in this chromospheres are selectively enhanced by a factor of 10^3 to 10^5. This selectivity is important not only for identifying vibrations of this particular chromospheres in a complex spectrum, but also for locating its electronic transitions in an absorption spectrum (Ferraro, J.R., 2003). According to the quantum mechanical theory of light scattering, the intensity per unit solid angle of scattered light arising from a transition between ground

state (m) and final state (n) is given by the standard expiration (Ferraro, J.R., 2003):

$$I_{mn}=\text{const } I_0 (w_0 - w_{mn})^4 \sum_{p\sigma}[(\alpha_{p\sigma})_{mn}]^2 \qquad (2.13)$$

Where 1_0 is intensity of the incident light of frequency, w_0 and $(\alpha_{p\sigma})_{mn}$ represents the change in polarizability α as a result of the electronic transitions m- e - n and, p and σ are x, y and z components of the polarizability tensor. This term can be rewritten as

$$(\alpha_{p\sigma})_{mn} = 1/h \sum \frac{MmeMen}{wen - w0 + iTe} + \frac{MmeMen}{wen + w0 - iTe} \qquad (2.14)$$

Where w_{em} and w_{en} are the frequencies corresponding to the energy differences between the states subscribed and h is Planck's constant. M_{me}, M_{en}, are the electric transition moments, such as

$$M_{me} = \psi^*_m u_\sigma \psi_e dt \qquad (2.15)$$

Here, ψ_m and ψ_e are total wavefunctions of the m and e states, respectively, and u, is the component of the electric dipole moment. Te is the bandwidth of the eth state, and the iTe term is called the damping constant. In normal Raman scattering, w_o is chosen so that $w_o \ll w_{em}$ Namely, the energy of the incident beam is much smaller than that of an electronic transition. Under these conditions, the Raman intensity is proportional to $(w_o - w_{mn})^4$. As w_o approaches w_{em}, the denominator of the first term in the brackets of eq (2.14) becomes very small. Hence, this term ("resonance term") becomes so large that the intensity of the Raman band at $w_0 - w_{mn}$ increases enormously. This phenomenon is called resonance Raman (RR) scattering (Ferraro, J.R., 2003).

2.4.2: Non-Linear Raman Effects

When a sample is illuminated with radiation which has an adequately large irradiance, some nonlinear optical processes may appear. For example, when the incident radiation has consisted of one monochromatic wave of frequency ω_0, the scattered radiation may include additional frequencies of the type $2\omega_0$ (hyper-Rayleigh radiation), $2\omega_0 \pm \omega_M$ (hyper-Raman radiation), $3\omega_0$ (second hyper-Rayleigh radiation), $3w_0 \pm \omega_M$ (second hyper-Raman radiation), etc

(Kumar, S., 2006). Analytical applications of such nonlinear Raman techniques are still rare and have been slow in coming, due largely to the complexity of the instrumentation, non linear Raman scattering can be also realized when the incident radiation consists of two or more overlapping coherent monochromatic beams, as in the case of coherent anti-Stoke Raman spectroscopy (Long, D.A., 2002).

2.4.3: Coherent Anti-Stoke Raman Spectroscopy (CARS):

CARS have become the most extensively used nonlinear Raman technique. In a typical CARS experiment, the incident radiation consists of two overlapping coherent monochromatic beams of frequencies ω_1 and ω_2, ($\omega_1 > \omega_2$) When $\omega_1 - \omega_2 = \omega_M$, where ω_M is a molecular frequency that can be observed in "normal" Raman scattering (Long, D.A., 2002). If we vary ω_2 while keeping ω_1 constant we find that the intensity of the scattering of the radiation with the frequency $2\omega_1 - \omega_2$ increases dramatically. In the resonance condition $\omega_1 - \omega_2 = \omega_M$, the produced frequency $\omega_s = 2\omega_1 - \omega_2 = \omega_1 + (\omega_1 - \omega_2)$ $= \omega_1 + \omega_M$ has the form of an anti-stoke Raman frequency relative to ω_1. As this scattered radiation is coherent, it is called coherent anti-Stokes Raman scattering, or CARS, differs in many important respects from the "normal" Raman process. CARS radiation forms coherent, highly directional beam with small divergence. CARS spectroscopy has two important advantages: strong signal level and high spatial resolution (Long, D.A., 2002).

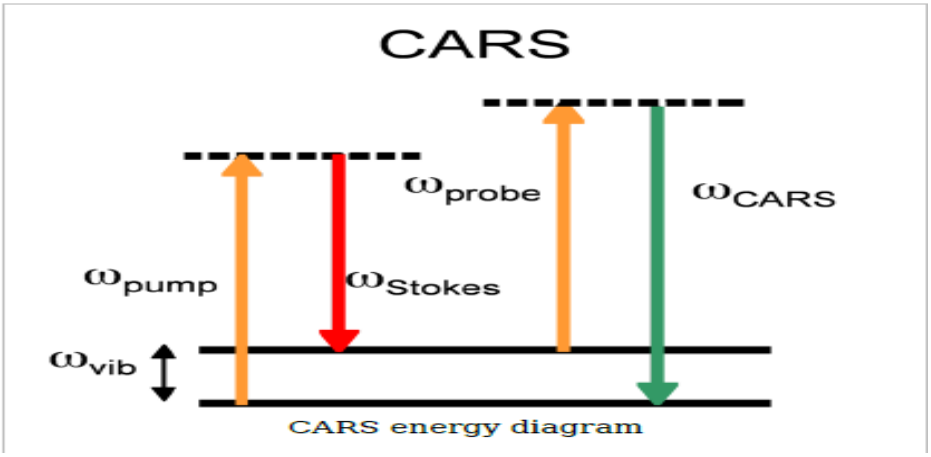

Figure (2. 3): Transitional scheme for CARS

2.4.4: Hyper Raman Effect

In hyper Raman spectroscopy, an intense beam of radiation is focused onto the sample. This is usually achieved using a 1064nm Nd YAG laser. If sufficient power is present and two photons interact with the one molecule then a virtual state is created at double the frequency of the laser excitation. Raman scattering from this virtual state to an excited vibrational state of the ground state is called hyper Raman scattering (Smith, E. and Dent, G., 2005).

2.4.5: FT-Raman Spectroscopy

With the idea that fluorescence may be reduced by shifting the exciting wavelength to longer wavelength, a new Raman technique, FT-Raman spectroscopy, was suggested in the 1960s and became viable in the 1980s. Employing an exciting line in the near-IR region from Nd:YAG laser (1064 nm) where electronic transitions are rare, FT-Raman is very effective in reducing or eliminating fluorescence interference for many samples. FT-Raman spectroscopy can also achieve high resolution, which is difficult for conventional Raman spectroscopy. Conventional Raman spectroscopy measures intensity vs. frequency or wavenumber.

FT instruments, on the other hand, measure the intensity of light of many wavelengths simultaneously. The latter is often referred to as a time-domain spectroscopy. This spectrum is then converted to a conventional spectrum by means of Fourier transformation using computer programs (Li, C. and Wu, Z., 2003). An optical diagram of a typical FT-Raman spectrometer is shown in figure (2-4). It may be observed that the laser radiation from Nd: YAG laser is passed through a band pass filter to remove non-lasing wavelengths is directed to the sample by means of a lens and a parabolic mirror, and the scattered light from the sample is collected and passed to a beam splitter and to the moving and fixed mirrors in the interferometer head. It is then passed through a series of dielectric filters and focused onto indium gallium arsenide

(InGaAs) detector or a liquid-nitrogen-cooled detector (Ge). Although the interest in FT-Raman has increased significantly, several limits of its capability remain: (a) FT-Raman cannot completely eliminate the fluorescence background when samples absorb light strongly in the NIR region. (b) The sensitivity of FT-Raman spectroscopy is still low since the Raman scattering cross-section decreases as E increases $(I \sim 1/E)^4$ although FT technique can improve the sensitivity somewhat. (c) It will not detect parts per million (ppm) impurities through spectral subtraction. (d) A serious problem of FT-Raman is the difficulty to study samples at temperatures >150°C. The thermal blackbody emission from the sample becomes more intense (broad background) than the Raman signal. The S/N ratio is lowered, and the detector becomes saturated (Ferraro, J.R., 2003).

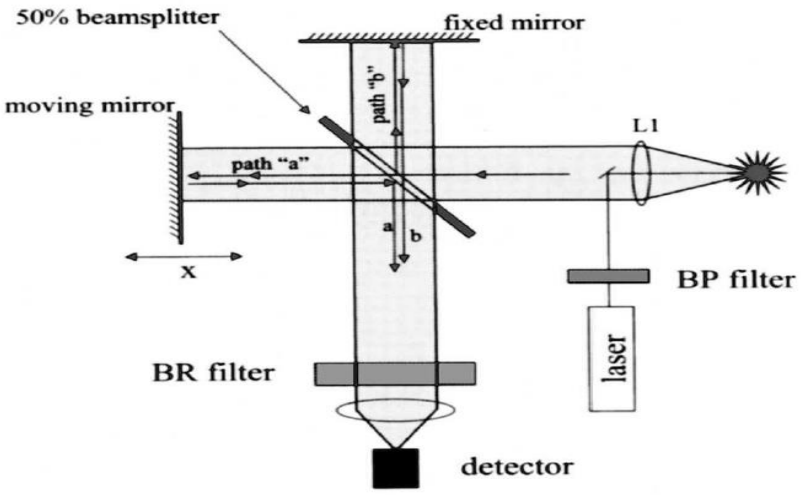

Figure (2.4): Schematic diagram of an FT-Raman spectrometer

2.4.6: UV Raman Spectroscopy

As the fluorescence usually occurs in the visible or near-UV region, UV Raman utilizes an excitation laser line in the UV region, which shifts the excitation wavelength to the opposite direction of FT-Raman. It has been demonstrated that there are several advantages of UV Raman spectroscopy over conventional Raman spectroscopy: (a) the fluorescence is avoided successfully in the UV region because most fluorescence appears in the visible region. (b) Increased sensitivity can result from UV excitation, since

Raman scattering efficiency is proportional to λ^{-4}, where λ is the laser wavelength. Thus, Raman scattering at 325 nm gas example, is a factor of 14 more efficient than that at 633nm.(c) With certain samples, UV laser excitation can interact in ways not possible when using visible laser sources. For example, in semiconductor materials the penetration depth of UV light is typically in the order of a few nanometers, and thus UV Raman can be used to selectively analyse from a thin top surface layer. In another example, UV excitation can give rise to specific resonance enhancement with biological moieties, particularly protein, DNA and RNA structures. Specific analysis of these materials within tissue can be difficult using visible laser wavelength (d) High excitation frequency leads to an important advantage when conducting high temperature in situ Raman experiments: the higher the excitation frequency, the lower the black-body radiation background (Li, C. and Wu, Z., 2003).

2.5: Experimental Techniques for Raman Spectroscopy

The basic configuration and components of a dispersive Raman spectrometer are the laser excitation source, sample illumination and collection optics, a spectrometer and a detector figure (2.6).

2.5.1:-Excitation Source

Raman scattering is inherently weak and is difficult to observe without intense monochromatic excitation and a sensitive detector modern Raman spectrometer system are nearly always use lasers as excitation source because their high intensity is necessary to produce Raman Scattering of sufficient intensity to be measured with a reasonable signal to-noise ratio. There are three types of lasers that operate in the ultraviolet (UV), visible and near-infrared regions Five of the most common lasers along with their Wavelength (nm) used for Raman spectroscopy are; Argon ion (488 or 514.5 nm), Krypton ion (530.9 or 647.1 nm), Helium / Neon (632.8 nm), diode laser (782 or 830 nm) and Nd-YAG (1064nm). Because the Intensity of Raman

scattering various as the fourth power of the frequency chosen for the exciting laser. Argon and krypton ion sources that emit in the visible region of the electromagnetic spectrum. Diode and Nd-YAG laser emit near-infrared radiation are used as powerful excitation sources. The Nd-YAG laser can be frequency doubled (half the wavelength, 532nm). Near-infrared sources have two major advantages over shorter wavelength lasers. The first is that they can be operated at much elevated power (up to 50W) without causing photo decomposition of the sample and secondly less fluorescence (Ferraro, J.R., 2003).

2.5.2:.Sample Illumination and Scattered Light Collection System

There are two basic geometries used in collecting Raman scattering: 90° and 180° scattering, geometries illustrated in Figs. 2-5a and 2-5b, respectively (Ferraro, J.R., 2003).

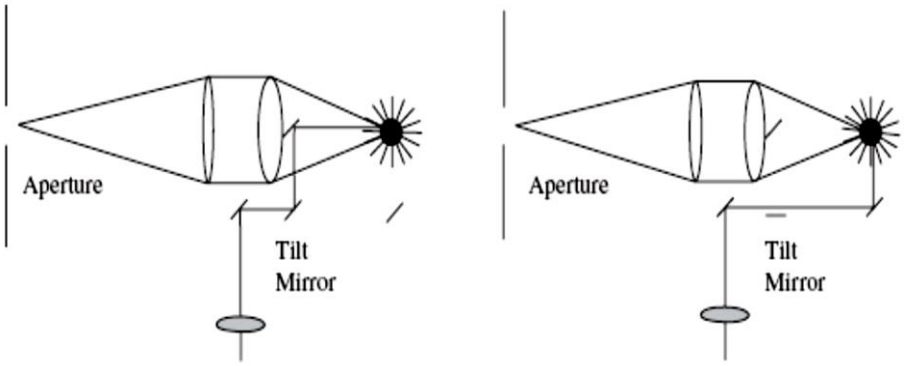

Figure (2.5): Configurations for (a) 90° and (b) 180° scattering geometries

In 90^0 scattering, the laser beam is passed through the sample, say in a 1cm cuvette, and the scattered light is collected at 90 by placing a lens in a suitable position. This light is then imaged onto the entrance slit of the Raman spectrometer. Since the light is scattered as a sphere, the larger the cone of light which can be collected the better. Consequently quite large lenses, or lenses with short focal lengths, are used to cover the largest practicable angle. It has to be remembered that this is not the only consideration. It is also necessary to use the monochromator efficiently and to image the collected light efficiently onto the detector As a result; the collection lenses have to be

matched to the collection optics for efficient performance (Smith, E. and Dent, G., 2005).

In the 180^0 system, the laser is delivered through the collection lens and the scattered light collected back through it. a small mirror is placed In front of the collections lens to achieve this. This is the common arrangement in systems which use a microscope to collect the light. Sometimes mirror systems such as a cassegranian system or a silvered sphere are used but lenses are more common. 'Grazing incidence' in which the laser beam is directed along the surface is sometimes used in special circumstances. Some years ago, the spectrometers were quite large (Smith, E. and Dent, G., 2005, Ferraro, J.R., 2003).

2.5.3: Sample Preparation and Handling

Raman spectroscopy, as a scattering technique, is well known for the minimum of sample handling and preparation that is required. Many organic, and inorganic, materials are suitable for Raman spectroscopic analysis. These can be solids, liquids, polymers or vapours (Smith, E. and Dent, G., 2005). The majority of bulk, industrial laboratory samples is powders or liquids and can be examined directly by Raman spectroscopy at room temperature. Accessories for examination of materials by Raman spectroscopy are available across a wide range of temperature and physical forms. Sample presentation is rarely an issue in Raman spectroscopy of bulk samples. Many materials can be mounted directly in the beam as neat powders, polymer films; etc. The sample could be taken in glass containers or capillaries tube. Raman spectroscopy is less demanding of beam position, for qualitative work with bulk samples, as the radiation is scattered. However, the sample can be optimized in the beam, particularly necessary for quantitative studies, but the collection solid angle has to be considered. On some occasions the angle of the sample to the scattered beam, i.e. 90^0or 180^0, will lead to orientation effects. Crystalline samples should be considered from this point of view.

Rotating the sample holder in order to avoid fluorescence or burning. Fluorescence arising from an impurity can, in some cases, be burnt out by leaving the sample in the beam for a few minutes or overnight. This works because there is specific absorption of the light into the fluorophore so that it is preferentially degraded. However, particularly with coloured samples, absorption by the sample can cause degradation of the sample itself. Again this can be reduced by rotating the sample, or vibrated when measuring the sample in order to avoid overheating by laser (Smith, E. and Dent, G., 2005, Li, C. and Wu, Z., 2003).

2.5.4: Raman Microscopes:

On many modern Raman spectrometers, the sample is simply presented to a microscope which is an integral part of the spectrometer. The microscope has many advantages. Very small amounts of material. Further, it can discriminate against fluorescence from a sample matrix since only the chosen microscopic feature in the sample is irradiated at high power. Particularly when the microscope is set up confocally. This inherently simple technology has big advantages. Visible laser sources and optics are very good. The coupling of visible spectrometers to an microscope to separate the light collection at the sensing point from them detection system is extremely efficient. Figure (2-6) shows a typical arrangement for a microscope. In this arrangement, the laser is focused through a pinhole and then collected as an expanded parallel beam. The reason for doing this is to fill the optics of the microscope. There is a plasma filter to remove any specious radiation such as weak emission from lines other than the main exciting line in the laser and any background radiation from the laser. The radiation is then arranged to hit a notch filter. These are interference filters, which work well when the beam is perpendicular to the plane of the filter. At the angle shown in the diagram, the laser radiation contacts the filter so that the light is entirely reflected into the microscope. Once the scattered radiation is collected from the microscope

back through the same optics, the beam is incident on the filter at the ideal angle for transmission of the scattered radiation. This light is then passed into the monochromator as shown and onto the CCD detector. Raman spectrometers also have polarizing optics before and after the sample. Another common choice of collection system, owing to the flexibility of fiber optics, is a small probe, designed to exciten the sample, coupled to a remote monochromator and detector to collect the scattering (Smith, E. and Dent, G., 2005).

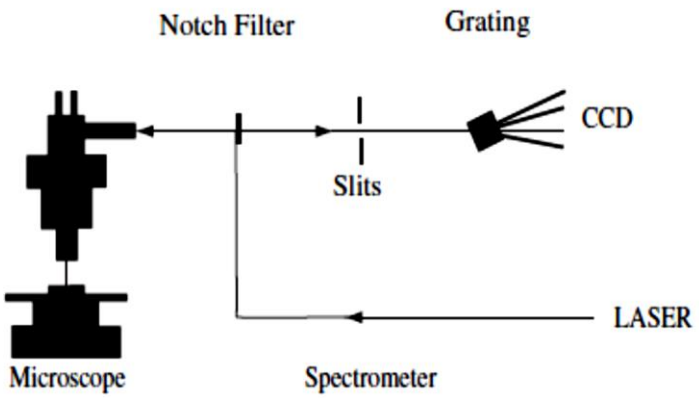

Figure (2.6): Raman spectrometer and microscope, using a visible laser, notch filter, and spectrometer and CCD detector

2.5.5: Filters in Raman Technique

Liquid filters are placed between the source and the samples tube. Different filters are used for different excitation radiation. Filters made of quartz glass or nickel oxide glass is used for getting monochromatic radiations. The functions of filters are; to isolate a single exciting line, to remove high-energy radiation that might cause photo decomposition or fluorescence, remove the continuous spectrum in the region occupied by the Raman lines, background interference in Raman data and also to reduce light attenuation caused by fiber absorption (Li, C. et al. 2003).

2.5.6: Monochromator and Detection System

To collect Raman scattering effectively it is necessary to remove the much more intense Rayleigh scattering and other light such as specula reflection from the surface of the sample. This light is much more intense than standard Raman scattering and can flood the detector especially if it is intended to detect Raman scattering which is close in energy to the laser frequency. Consequently some device has to be employed to separate the wavelength shifted Raman scattering from the other light collected. This can be done with two or even three monochromators. The purpose of the first monochromator is mainly to separate the frequency-shifted Raman scattering from the other radiation. The second monochromator increases the dispersion and separates the individual Raman peaks. The radiation is then focused onto a CCD. That can measure the intensity of light at different frequencies (Esmonde-White, K.A., 2009, Manoharan, R. and Sethi, N., 2003).

2.5.7: Computer

A computer and its associated software are used with Raman microscope spectrometer for two main purpose the first function include, instruments control, spectral data collection, data processing and analysis the second function its used to provide automation of data collection and component prediction process (Lewis, I.R. and Edwards, H., 2001).

2.5.8: Operational Parameters

There are number of operational parameters that influence the quality of the Raman spectrum obtained from the sample which have been significant in the current study. These parameters include laser power, recording time and number of accumulations (Legodi, M.A., 2008).

2.5.8.1: Laser Power

This parameter affects the shapes and intensities of the bands resulting from the sample under investigation. The increase in laser power may result in band broadening and shifts. These effects arise from local heating due to

relatively high laser power, which enhances an harmonic interactions. The increase in laser power may destroy the sample or transform it into a different chemical phase. The laser power may range from a few mill watts (0.1 mW) to several hundreds. For the heat sensitive compounds e.g. pigments, low laser powers (5 mW) are desirable in order to minimize the possibility of sample degradation. Colored molecules can be so strongly absorbing that they thermally degrade. At lower laser power, no sample heating is observed but the spectrum is very weak. As the laser power is increased the Raman band intensities may increase but the baseline starts to increase at high Raman shift because of the effect of sample heating (Lewis, I.R. and Edwards, H., 2001).

2.5.8.2 Sample Recording Time

Some compounds, e.g. silicates, are weak Raman scatterers and short time recordings may not yield any peaks. However, with longer recording times the results improve. Therefore, the extension of recording time increases the efficiency and sensitivity of Raman spectroscopy. However, for heat sensitive samples degradation may occur as the recording time is lengthened (Lewis, I.R. et al 2001).

2.5.8.3: Number of Accumulations

Instead of increasing the acquisition time several spectra can be accumulated to increase the signal to noise ratio. In general it is less time consuming to increase the acquisition time than to accumulate spectra. However, accumulating spectra is the only way to generate a better signal to noise ratio (McCreery, R.L., 2005).The recordings using more accumulations result in more pronounced Raman peaks. However, increasing the number of accumulations can result in a different spectrum. This is a direct result of sample heating capacity and/or the heat capacity of its surroundings (Lewis, I.R. and Edwards, H., 2001).

2.6: Advantages and Disadvantages of Raman Spectroscopy

Raman spectroscopy has a number of advantages, but also some disadvantages compared to other methods. Advantages include the following:

1- Wide variety of acceptable sample forms: Samples for analysis may be solids, liquids, or gases, or any forms in between and in combination, such as slurries, gels, and gas inclusions in solids. Samples can be clear or opaque, highly viscous or liquids with lots of suspended solids. While this variety is easy for Raman spectroscopy, it would be challenging for mid-IR and near-infrared (NIR) spectroscopy and numerous non-spectroscopic approaches.

2- No sample preparation, conditioning, or destruction: Little or no sample preparation is required for Raman experiments. Which is particularly valuable in a process installation. Most process implementations are designed to require no sample conditioning. The sample is not destroyed during the experiment, except for a few cases like black or highly fluorescent materials or materials that absorb enough lasers light to be thermally degraded (Lopes, J.A., 2005)

3- A rapid method. High quality Raman data are acquired in very short periods of time, often within seconds. E. g. chemical analyses generally take minutes or even hours. This kind of analysis definitely spares time. The rapidity of the method yields further potentialities inherent in a scope of almost immediate response and quasi real time processes e. g. chemical changes kinetics monitoring.

4- Non-destructive. Sample can be after Raman analysis consequently treated by other procedures. Non-destructiveness also enables potential as in-vivo diagnostic tool in medicine providing information about both the chemical and morphologic structure of tissue in quasi-real time (Vašková, H., 2011).

5- Stable and robust equipment. Most process Raman instruments have few moving parts, if any, and thus are quite stable and robust. This also reduces the number of parts likely to need replacement (Lopes, J.A., 2005).

6- Measurements of depolarization ratios provide reliable information about the symmetry of a normal vibration in solution. Such information cannot be obtained from IR spectra of solutions where molecules are randomly orientated (Ferraro, J.R., 2003).

7- Water is a weak Raman scatter, Raman spectra of samples in aqueous solution can be obtained without major interference from water vibrations. In contrast, IR spectroscopy suffers from the strong absorption of water – or no special accessories are needed for measuring aqueous solutions (Ferraro, J.R., 2003).

8- Raman spectra of hygroscopic and/or air-sensitive compounds can be obtained by placing the sample in sealed glass tubing. In IR spectroscopy, this is not possible since glass tubing absorbs IR radiation (Ferraro, J.R., 2003).

9- Raman vibration information tends to appear as sharp peaks than IR vibration Spectroscopy, IR vibration are influenced by hydrogen bonding effect that broaden infrared peaks, where Raman peaks are not typically influenced by these effect (Kiefer, J., 2015).

10- The standard spectral range reaches well below 400 cm^{-1}, making the technique ideal for both organic and inorganic species (Amer, M. ed., 2009).

On the other hand, disadvantages include:

A. Laser source is needed to observe weak Raman scattering. This may cause local heating and /or photodecomposition, especially in resonance Raman studies where the laser frequency is deliberately tuned in the absorption band of the molecule (Ferraro, J.R., 2003).

B. Some compounds fluoresce when irradiated by the laser beam. (High background signals to reducing this problem, including using longer laser wavelengths and summing numerous short acquisitions (Ferraro, J.R., 2003).
C. It is more difficult to obtain rotational and rotation-vibration spectra with high resolution in Raman than in IR spectroscopy. This is because Raman spectra are observed in the UV-visible region where high resolving power is difficult to obtain (Ferraro, J.R., 2003).
D. The state of the art Raman system costs much more than a conventional FT-IR spectrophotometer although less expensive versions have appeared which are smaller and portable and suitable for process applications (Ferraro, J.R., 2003).
E. Interference from laser-induced fluorescence or impurities in the sample may be a problem in some applications. In order to avoid such effects a number of approaches have been developed including near-infrared Raman, UV Raman, polarization-resolved detection Raman, and surface enhancement Raman spectroscopy (Kiefer, J., 2015).
F. Accurate gas-phase measurements often require high power laser sources in order to generate sufficient signal photons (Kiefer, J., 2015).

2.7: Applications of Raman Spectroscopy:

As Raman spectroscopy is a branch of vibrational spectroscopy and provides fingerprints for various types of molecular systems due to its very specific vibrational information about the chemical bonds in molecules. The spectral acquisition can be done in seconds; this makes Raman spectroscopy a fast analytical tool in vibrational spectroscopy. This technique provides rich information content at high speed of analysis, needs only minimal sample preparation, and mostly uses simple experimental setups. The introduction of the laser and modern developments, increased Raman spectroscopy has become a tool for not only purely research but also be more accessible in

different application fields including material science, chemistry, physics, industry, biology, geology, and medicine (Hassanein, R., 2011).

2.7.1: Industrial Applications

Raman spectroscopy is becoming interest in industrial applications specialty chemicals, petrochemicals, petroleum refining, pharmaceutical, food, and paper since the advents of FT-Raman instrumentation, fiber optics and detectors. These three factors have synergized and have led to the present interest in Raman spectroscopy. This has brought the Raman effect from the laboratory and into the plant, where in-situ measurements are now possible in a number of industrial environments (Ferraro, J.R., 2003).

2.7.1.1: Food Industry:

Raman spectroscopy is emerging as a fast tool for quality control and adulteration detection. Moreover, it is also used to detect changes that occur during food processing or measurements of fatty acid un saturation in different types of vegetable oils (e.g. olive oil, coconut, corn, sunflower, peanut, palm, rapeseed and soybean) as well as animal fats, such as butter and tallow have been analyzed by FT-Raman spectroscopy (Hassanein, R., 2011). The presence of double bonds C=C in the unsaturated fatty acids in lipids provides a method of determining instauration. It indicates the un saturation level of the fat-containing food Products. The higher the iodine value, the greater the un saturation (Chatgilialoglu et al.2013).

2.7.1.2: Dye Industry:

FT-Raman and a micro FT-Raman instrument its powerful tool to investigation low levels of dyes or dyestuffs in acrylic fibers. The acrylic fibers which its often copolymer of about an acrylonitrile (94%) and methacrylate(6%) with a diameter of 12-20 microns. The cell used for the measurement is illustrated in figure (2.8), resolution $3cm^{-1}$ and 50-150scans.

Figure (2.10) show the vibrations of three different dyes, a blue dye fiber, red dye fiber and an un dyed meth acrylic fiber. The vibrations spectrum of the dyed observed and fiber the spectral subtraction procedure was used (blue dyed fiber minus the un dyed fiber). The subtraction spectra provide valuable

information on the nature of the dye and can be compared with spectra of pure dyes (Ferraro, J.R., 2003).

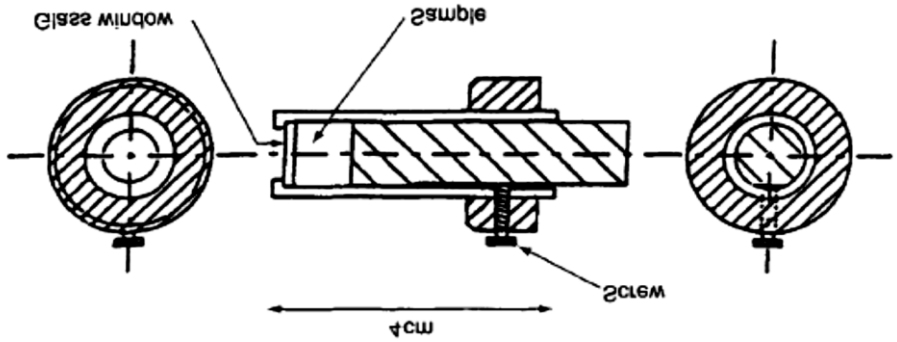

Figure (2-7): Fiber cell used for recording FT Raman spectra of fibers of dyes.

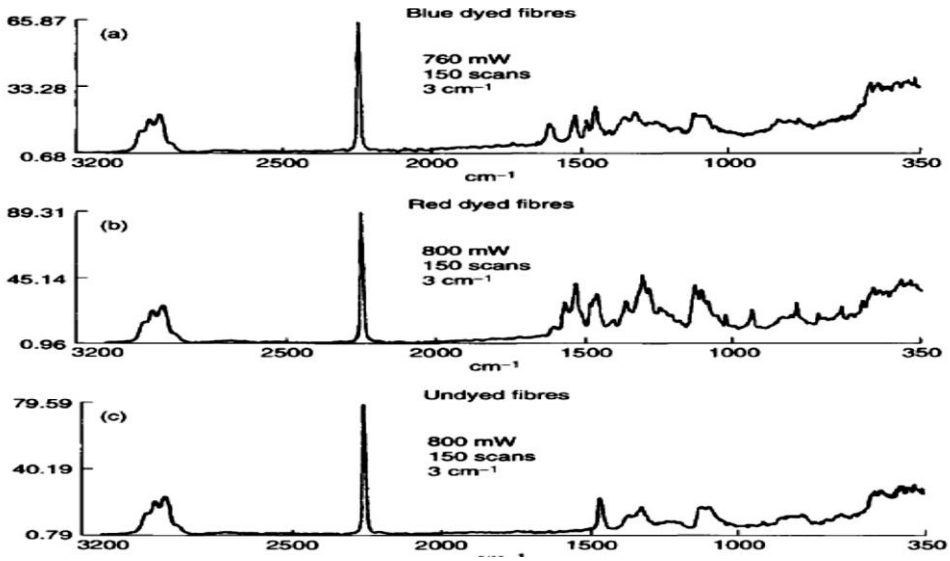

Figure (2-8): FT Raman spectra of acrylic fibers: (a) blue-dyed, (b) red-dyed, (c) un dyed

2.7. 2: Biological Applications

Raman spectroscopy has been applied broadly to biological molecules, especially to probe the structure and function of proteins not only on the aromatic amino acids phenylalanine, tyrosine and tryptophan, the S-S and S-H groups of cystine and cysteine, the C-H groups of aliphatic amino acids, the COO- and COOH groups of aspartic and glutamic acids, and the imidazole ring of histidine., but also on the peptide bonds via the amide as (amide I), (amide II), (amide III), (amide IV), (amide V) and, (amide V I)and (amide S). Bands corresponding to the amide I, amide III and amide S stretching modes

can be used to characterize backbone conformation and giving information on the relative proportions of different types of secondary structures in polypeptides or proteins such as a-helix, B-sheet and random coil (Ferraro, J.R., 2003). The use of 180^{o} scattering with the development of microscopes and microprobes has led to automation for fast screening and the ability to examine systems in situ. In the case of microprobes, the enhancement techniques such as SERS and SERRS which can use metal colloids as part of the probe have brought large increases in sensitivity. The researchers have used these techniques, to detect DNA, and along with other approaching single molecule detection. Among a vast number of applications reported are binding studies, genomics, lab on a chip, proteomics, protein interactions and solid phase synthesis. DNA and protein arrays as well as cell growth have been studied. There are also a large number of published studies in the food and biomedical fields. A few examples are, transitions in amino acid crystals, single-cell bacteria, bacterial spores, carotenoids in numerous systems including Atlantic salmon, characterization of microorganisms, fungi, grain composition, liposome complexes, yeast and benign and malignant tissue in thyroid and human breast tissues. Specific studies of chromophore containing proteins can give good structural information from suspensions as illustrated for P450 enzymes. Gradually, as equipment and skill improves through the work of some excellent groups, Raman scattering is becoming a useful technique in medicine (Dent, G. and Smith, G., 2005).

2.7.3: Medical Applications

There are several Raman active biological molecules in tissue that give distinctive peaks in the spectrum giving structural and environmental information about the tissue. The changes in tissue that occur as a result of a disease yield a characteristic Raman spectrum that can be used for diagnosis. Several in vivo tests have to be done, to fully evaluate the actual usefulness of Raman spectroscopy. Raman spectroscopy has been studied extensively for

tissue diagnosis on skin, breast, esophagus, cervix, lung, throat, etc. Besides Raman spectroscopy, several other optical techniques are being developed for the same applications, such as diffuse use reactance spectroscopy, fluorescence spectroscopy, photoacoustic and diffuse optical tomography. The main advantage of Raman spectroscopy is that tissue consists of many Raman active molecules such as in Skin cancer diagnostics, and Breast cancer diagnostics which have distinctive spectral signatures (Naglic, P., 2012).

2.7.4: Applications of Chemistry

Raman spectroscopy provides a chemical fingerprint for identification of a molecule, since vibrational information is specific to the chemical bonds and symmetry of molecules. not including for identification the method is used for characterization and analyses of organic and inorganic substances, including carbon materials, solvents, and films and for chemical processes monitoring (Vašková, H., 2011).

2.8: Literature Review

D. L. A. de Faria, S. Venaü ncio Silva and M. T. de Oliveira used Raman microspectroscopy in 1997 to indentify some iron oxides and oxyhydroxides. Raman microscopy was employed to investigate the laser power dependence of the spectra of these oxides and oxyhydroxides. Low laser power was used for the reference spectra in order to minimize the risks of spectral changes due to sample degradation. The results obtained show that increasing laser power causes the characteristic bands of hematite to show up in the spectra of most of the compounds studied whereas the hematite spectrum undergoes band broadening and band shifts. They report investigations of the Raman spectra of hematite (Fe_2O_3), magnetite (Fe_3O_4), wustite (FeO), maghemite (γFe_2O_3), goethite (αFeOOH), lepidocrocite (γ-FeOOH) and δ-FeOOH in order to clarify the influence of laser power on the Raman spectra. The spectra were obtained directly from powdered samples with very low laser power (0.7 mW), minimizing the problems caused by sample handling. The Raman

equipment was a Renishaw Raman imaging microscope. The spectra were excited by focusing He-Ne laser on the sample with 632.8 nm at power 0.7 mW at the sample, to avoid sample degradation then raising the laser power to 7 mW (at the sample) causes the bands to broaden and to undergo a small shift to lower wavenumbers, as shown in Table (2.2) in hematite as example.

Table (2-2): Wavenumbers (cm^{-1}) and full widths at half maximum (FWHM) for hematite as a function of laser power

Laser power 0.7mW		Laser power 7mW	
Raman shift/ cm^{-1}	FWHM/ cm^{-1}	Raman shift/ cm^{-1}	FWHM/cm^{-1}
226.7	4.8	219.6	10.2
245.7	6.0	236.5	22
292.5	7.1	282.7	20
299.3	8.5	295.2	17.3
410.9	11.6	395.9	29.3
497.1	21.2	492.3	51.9
611.9	14.4	596.0	38.9

In 2009, Monika Hanesch used Raman spectroscopy to indentify iron oxides and oxihydroxides at low laser power to investigate the possible applications in environmental magnetic studies. Raman spectroscopy of synthetic and natural iron ox hydroxides and iron oxides was performed to test its potential in environmental magnetic studies and soil science. The main aim was to distinguish between the different iron oxides occurring in soils. Most of them can be identified by magnetic methods, but there are some minerals that are not easy to differentiate from each other. In these cases, the magnetic methods can be complemented by Raman spectroscopy. Raman spectra were obtained using 100mW frequency doubled Nd-YAG laser with 532.2 nm and diffraction gratings of 1800 grooves mm^{-1}. Laser power can be reduced by filters to 1, 0.1 and 0.01 mW. Due to the low laser powers applied, a wuestite band appeared at 595 cm^{-1}, Magnetite band appeared at 310 cm^{-1}, 540 cm^{-1},

and 670 cm^{-1} maghemite bands appeared at 350 cm^{-1},512 cm^{-1} and 665 cm^{-1}, goethite band appeared at 244 cm^{-1}, 299 cm^{-1}, 385 cm^{-1},480 cm^{-1}, 548 cm^{-1} and 681 cm^{-1} additionally other materials appeared like TiO_2, at 142 cm^{-1} and 516 cm^{-1}.' hematite bands appeared at 225 cm^{-1} 245 cm^{-1},290–300 cm^{-1}, and 412 cm^{-1}, also lepidocrocite bands appeared at 250, 348, 379, 528 and 650 $cm^{-1,}$ and ferrihydrite bands appeared at 370, 510 and 710 cm^{-1} could be established also enabling a non-ambiguous identification of this mineral by its Raman spectrum. Furthermore, the potential of the method to investigate magnetic material produced by soil bacteria is demonstrated.

M.A. Legodia and D. de Waalam used Raman spectroscopy in 2007, for the preparation of magnetite, goethite, hematite and maghemite of pigment quality from mill scale iron waste. Magnetite and goethite were precipitated from their respective precursors in aqueous media. Various red shades of hematite were prepared by the calcinations of the precipitated goethite at temperatures ranging from 600 to 900 °C. Maghemite was obtained by thermal treatment of magnetite at 200 °C. The iron oxides were characterized by Raman spectroscopy, X-ray diffraction (XRD), surface area determination and scanning electron microscopy (SEM). Raman spectra were recorded at room temperature using a Dilor XY Raman spectrometer with a resolution of 2 cm^{-1}. Radiation at 514.5 nm from an Ar+ laser was used to excite the samples. The laser power was set at 100 mW at the source. The recording time was set between 30 and 180 s, with two accumulations per spectrum segment. An Olympus Mplan 100X objective on an Olympus BH-2 microscope was used to focus on the sample. The Raman spectra were analyzed, Magnetite spectra appeared at 297, 666 and 523 $cm^{-1,}$ goethite bands appeared at 223, 297, 392, 484, 564 and 784 cm^{-1} hematite characteristic bands appeared at 226, 292, 406, 495, 600 and 700 cm^{-1} and Maghemite 358, 499, 678 and 710 $cm^{-1.}$.

In 2012, A F. Betancur, F. R. Pérez, M. del M. Correa, C. A. Barrero used infrared and Raman Spectroscopy in quantitative analysis in iron oxides and oxihydroxides.

Raman and infrared spectroscopic measurements were carried out. For both sets of spectrum, mathematical relationships between the Raman and Infrared fraction, as obtained from the characteristic bands of each phase, and the respective mass fraction, were established. In most cases, linear relationships were obtained. A problem sample was used in order to estimate their respective relative phase abundances obtaining better results from the Raman spectroscopy measurements.

In Raman spectroscopy: The most representative bands of hematite are around 228.6 $cm^{-1}$and 295.02 cm^{-1}. According to Faria et al, these bands of hematite are two of the seven Raman active phonons. These two bands were taken for quantitative analysis. The remaining five phonon bands at about 247.9, 300.9, 413.8, 500.2 and 614.5 cm^{-1}, all of them were found in our spectrum. From the literature, the band at about 1317.8 cm^{-1} is a vibration which has some unclear origin. Faria et al , says that this band is caused by the scattering of two magnons in the structure, but according to Su *et al.*, this phonon consists in a second harmonic vibration. It is important to say that the band of hematite at 1317.8 cm^{-1} is close to the magnetite at approximately 1304.9 cm^{-1}. This causes an overlapping in vibrations when these two phases are mixed, making difficult their identification by using those bands. Therefore, these bands were not selected as analytical bands of hematite and magnetite. The band of goethite that stands out over other active modes in Raman spectra is 388.8 cm^{-1}. The band at about 552.3 cm^{-1} does not appear in the other analysed phases, therefore, it was used for the development mathematical fitting. In the case of magnetite, the most representative band is found at about 667.2 cm^{-1}, hence they selected it as the analytical band. The other bands cannot be selected, because they interfere with bands from the other phases.

Chapter Three

The Experimental Part

3.1: Introduction

In order to illustrate the ability of Raman spectroscopy to indentify the unstable compounds of iron oxides, laser Raman spectrometer model sentrra (Burker, Germany) equipped with an Olympus 100x long working distance microscope, was used. The parts of burker senterra micro Raman spectrometer are shown in figure (3.1) (Hassan, S.S et al 2015). The Raman spectra were recorded using 5mW frequency doubled Nd-YAG laser with 532 nm at room temperature. This chapter demonstrates and explains the experimental setup, materials and methods, instruments structure and experimental procedure used for the investigation of the unstable compounds in five samples of iron oxides which are: hematite, magnetite, goethite, akaganaite and ferrihydrite.

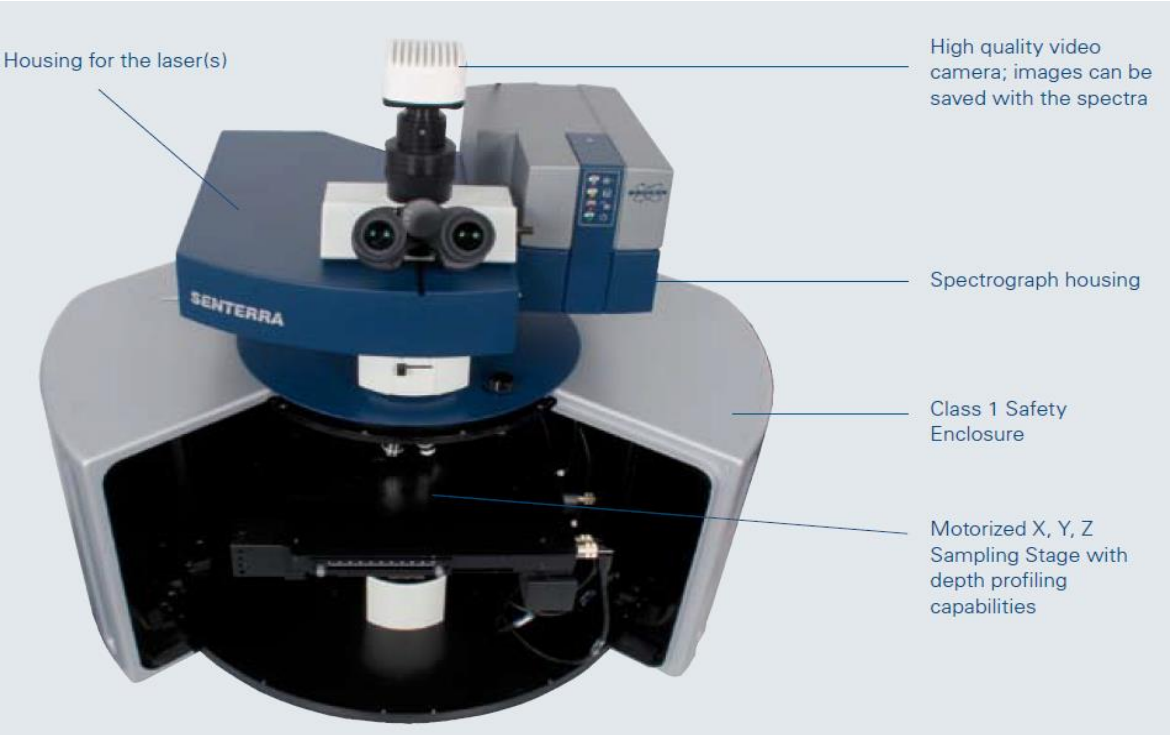

Figure (3.1): The parts of burker sentrra laser Raman microscope spectrometer

3.2 Instruments and Apparatus:

This part presents the substances of the Laser Raman microscope spectrometer model burker senterra instrument which was used in this work and its specifications in details. Burker senterra is a high performance Raman microscope spectrometer designed for demanding analytical applications and research applications. The senterra Raman microscope incorporates many features that make it the ideal choice for the analytical laboratory (Wang et al .2016).

1- High wavenumber accuracy
2- All-in-one, compact, confocal design
3- Removal of fluorescence background with Concave Rubber band correction multiple wavelength
4- Ft- Raman with1064nm excitations
5- High spatial and spectral resolution
6- Class 1 laser safety enclosure standard
7- Computer controlled xyz mapping stages with autofocus.

The optical device of the Raman microscope is based on the Olympus BX51 microscope

3.2.1: Structure of Raman Microscope Spectrometer

The basic configuration and components of burker sentrra laser Raman microscope spectrometer are consists of a standard optical microscope, an excitation laser, sample illumination and collection optics, monochromator and a sensitive detector (CCD) as shown in figure (3.2). The correct selection of the laser wavelength is an important consideration for Raman spectroscopy, several laser wavelengths may be employed to obtain the best detection limit of the Raman signal with sensitivity. Laser source with green region (532 nm), laser in the red (633 nm) or near infrared (NIR) (785 nm) region are the possible solutions for the Raman analysis. With the lower photon energy, a red or NIR laser may not promote the electronic transition

(and hence the fluorescence) and so the Raman scatter may be far easier to detect.

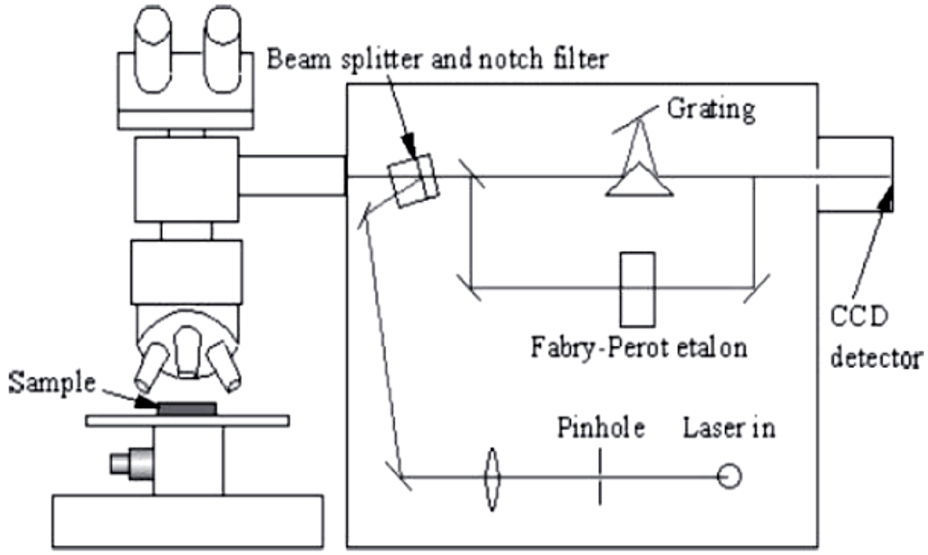

Figure (3.2): schematic structure diagram of burker sentrra laser Raman microscope spectrometer.

3.2.2: The Laser Source

The light source used in this spectrometer is frequency doubled Nd-YAG laser with wavelength 532nm and output power of 5mW.

3.2.3: The Optics

In a dispersive Raman spectrometer, the sample is positioned in the laser beam, and the scattering radiation is collected either in a 180° (the backscattering method) or a 90° (the right-angle method) scattering configuration. Beam splitter (the beam is split into 2 equal components by a silicon-coated copper fluoride beam splitter). Dispersive spectrometers are equipped with efficient light rejection filters to suppress the Rayleigh line and stray light. Frequently used filters Holographic notch filters have revolutionized Raman spectroscopy by providing excellent attenuation of the Rayleigh line while passing bands as near to it as 50 cm^{-1}. They also exhibit good transmission in both the Stokes and anti-Stokes line The notch filter has a narrow rejection band, typically 12 nm, which enables detection of low wave number shifts (~50 cm^{-1}) (Bakeev, K.A. ed., 2010).

3.2.4: Raman Microscope Analysis

Burker sentrra Raman spectrometer based on the Olympus BX series optical microscope spectrometer. Its high spatial resolution spectroscopy and imaging, typically using low laser power (<20mW) to minimize sample degradation or sample heating. A motorized X, Y and Z stage with a nominal resolution as small as 10 nm is used for scanning the surface for lateral and depth information. Raman spectral mapping complements the visual image obtained with the microscope by providing information about the variation in chemical or physical properties of a heterogeneous surface. Raman scattering measurements can be performed at room temperature using several laser sources 488 nm,, 532 nm, 633 nm, 785 nm, and 830 nm. (McCreery, R.L., 2005). To control of the depth of analysis by controlling the depth of focus, with hybrid aperture containing array of a pinhole for high confocal mode of operation and slit for high throughput with Flex Focus shown in figure (3.3). Using Flex Focus, a depth resolution of better than 2 μm is obtained with a 100x objective and the 50 μm pinhole. Lastly, by utilizing a single mount to have access to the high throughput and confocal modes of operation, the number of moving parts, as well as the beam path, is minimized and the throughput is therefore enhanced (Wang et al .2016).

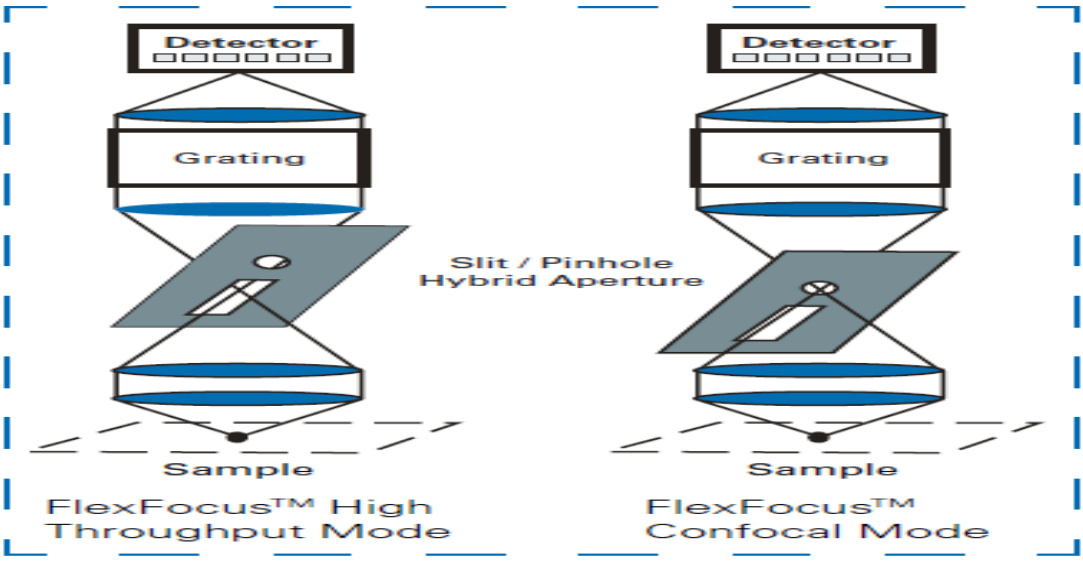

Figure (3.3): Schematic x-y-z stage with sample representation of the confocal Raman microscope adopted from reference

3.2.5: The Spectrograph

A typical spectrograph consists of mirrors and a grating for dispersion is the main part of this device. Ruled diffraction grating spectrographs use aluminum-coated optical surfaces and are not very efficient for NIR region. Further improvement in throughput is achieved by using gold-coated optical components. The development of holographic optics offers highly efficient holographic gratings for improved excitation light rejection with additional advantages such as fewer optical elements and compact size, and the light beam acceptance angle can be matched with that of the optical fibers for increased system throughput. The critical requirement of all spectrographs is temperature stability. The analyzer must be very well temperature controlled or located in a temperature-controlled environment (Manoharan, R. and Sethi, N., 2003).

3.2.6: The CCD Camera

The array detector used in the Raman holoprobe is a charge coupled device (CCD) detector. The popularity of CCDs arises out of the fact that they combine low noise, large dynamic range, and high quantum efficiency with the ability to store and measure charge in two dimensions thus having the capacity to represent images (Robertson, I., 2000). CCD camera consist of

two dimensional arrays of pixels (e.g., 256 1024) that each can be considered as an independent detector. The horizontal pixels are calibrated so as to correspond to the wave number axis, while the vertical pixels actually measure the strength of the Raman signal. In other words, the image on the CCD camera is an electronic picture of Raman signal that is then converted into spectrum (Sasic, S. ed., 2008). The number of electrons collected in a well is directly proportional to the number of photons incident on that pixel. The best signal to noise ratio is obtained when the exposure of the CCD detector allows the wells to nearly fill. The most significant source of noise in most CCDs is quantum or 'shot' noise. Shot noise arises from the random arrival times and energies of incident photons. Two consecutive spectral measurements of the same sample will always show some variation in the number of photons collected at any pixel. Longer collection times can reduce the relative levels of shot noise. Dark current and cosmic rays can also contribute to the production of inaccurate spectra. Dark current is a background external current that is produced even when there is no radiation incident on the detector and leads to a dark current curve. Cosmic rays are high-energy particles, originating from spaces that lead to spikes in the spectra. The contributions from both dark current and cosmic rays can be corrected for within the software package (Robertson, I., 2000).

3.3: Materials and Methods

Five samples of hematite, magnetite, goethite, akaganeite and ferrihydrite were investigated in this work by laser Raman spectrometer in the range from 50 cm^{-1} to 4500 cm^{-1}.

3.3.1: Samples Preparation

Samples were prepared as follows:

Sample 1: Hematite (Fe_2O_3)

Fourty grams of Ferric nitrate (Fe $(N0_3)_3$. 9 H_20) was dissolved in 500 ml of twice distilled water in polyethylene flask. Then, 300 ml of one molar (1M)

potassium hydroxide (KOH) was added to the flasked followed by 50 ml of one molar (1M) sodium bicarbonate ($NaHCO_3$). The mixtures were heated to $90C^0$, till formation of red brown precipitates of ferrihydrite. The flask and the content were allowed to stand for 48 hours. During this time the red brown suspension of ferrihydrite was transformed to hematite with pH of 8 to 8.5 (Schwertmann, U. and Cornell, R.M., 2008).

Sample 2: Magnetite (Fe_3O_4)

One molar of 1ml Ferric nitrate ($Fe(NO_3)_3 \cdot 9H_2O$) was dissolved in 10 ml of distilled water to form a transparent yellow solution. Next, three different mineralizing agents were added into the ferric solution ; First was 5 ml of 10.67 molar KOH aqueous solution added drop wisely into the ferric solution. Second was 1 ml of ethylenediamine (EDA). The EDA was added gradually into the ferric solution. Third was a combination of KOH and EDA. The 5 ml of KOH solution at molar 10.67 was added first, followed by 1 ml of EDA. After adding these mineralizing agents, a brown $Fe(OH)_3$ suspension was obtained. Then, these solutions were all stirred for 30 min before transferring the mixture into a Teflon-lined stainless steel autoclave of 40 ml capacity and followed by heat treatments at 200°C for 9 h. After that, the autoclave was cooled down to room temperature in air. The precipitates were collected by centrifugation, washed with ionized water and ethanol several times to remove organic and impurities, and finally dried in air at 80°C for 12 h (Lu, J.F. and Tsai, C.J., 2014).

Sample3: Goethite (αFeOOH)

100 ml of one molar (1M) Ferric nitrate ($Fe(N0_3)_3$ solution was added into 2 liter polyethylene flask, then 180 ml of five molar (5M) potassium hydroxide (KOH) was added rapidly with stirring, till the formation of red brown precipitates of ferrihydrite at once. The suspension was diluted with twice distilled water and holded in a closed polyethylene flask maintained at 70 C^0 in an oven for 60h. At the end of this period of time the red-brown suspension

of ferrihydrite was transformed in to a compact yellow precipitate of goethite (Cornell, R.M. and Schwertmann, U., 2003).

Sample 4: Akaganeite (βFeOOH)

0.1 molar (0.1M) of $FeCl_3$ solutions was hold in to 2 liter in closed vessel at 70 C^0 for 48h. During this time the pH of the system drops from 1.7 to 1.2 and compact yellow precipitate of akaganeite was formed (Cornell, R.M. and Schwertmann, U., 2003).

Sample 5: 2-Line Ferrihydrite

Fourty gm of Ferric nitrate(Fe $(N0_3)_3$. 9 H_20) was dissolved in 500 ml distilled water and added with stirring, 330ml 1molar KOH was added to bring the pH to 7-8, centrifuge, then dialyze rapidly as possible to remove electrolytes and freeze dry (Schwertmann, U. and Cornell, R.M., 2008).

3.3.2: The Experimental Procedure

Iron oxide samples were synthesized using Fe $(N0_3)_3$. 9 H_2 O and KOH with different molar ratios through the chemical method, the spectra properties of these samples were investigated in order to indentify the unstable compounds. Laser Raman spectra were collected at room temperature using burker sentrra micro Raman spectrometer. Frequency doubled Nd-YAG laser was used to excite the samples. The laser power was set at 5mW (is recommended; high power settings can burn samples, especially organic materials). The recording time was set at between 20 and 30 s. The powder samples employed were placed on the microscope stage of the Olympus confocal Raman microscope attached to the spectrograph. The radiation passes through pin holes and lens. The beam is directed to the microscope (Olympus 100X objective) via mirrors and then directed into the microscope via one beam splitter and holographic notch filter, which rejects any Rayleigh scattering. The backscattered Raman radiation is filtered through the spectrograph entrance and then onto the CCD detector and computer.

Chapter Four

Results and Discussion

4-1. Introduction:

This chapter presents the data collected from the experimental work, in figures, and tables. The data is analyzed and discussed. Raman spectra were recorded at room temperature using burker sentrra micro Raman spectrometer. The frequency doubled Nd: YAG laser 532.0 nm and output of power 5mW was used to excite samples of iron oxides. Raman spectra were collected over the wavenumber range (50 cm^{-1} to 4500cm^{-1}).

4.2: Results and Discussion

Figure (4.1) shows the Raman spectrum of hematite after irradiation with Nd-YAG laser. The spectrum shows clear peaks and by comparison with the vibrations recorded in some references we found that these vibrations are attributed to hematite compounds beside unstable components of hematite and some components of materials that are listed in table (4.1).

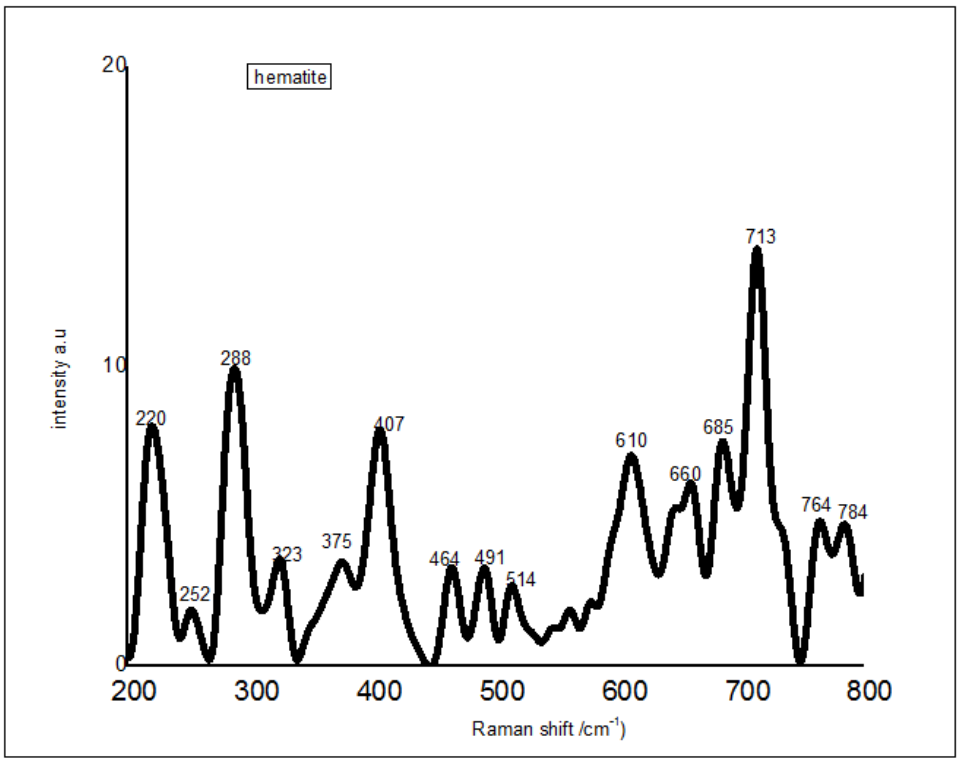

Figure(4.1): Raman spectrum of hematite in the range from 200 −800 cm^{-1}

Table (4.1): The analyzed data of Raman spectrum of the hematite

Raman shift (cm^1)	Intensity (a.u)	Assignment	References
220	8.51	FeII-O	[Thibeau et al. 1978, De Faria et al. 1997]
252	2.8	FeII-O	[Thibeau et al. 1978, De Faria et al.1997, Shebanova, O.N. and Lazor, P., 2003]
288	10.7	FeII-O	[Thibeau et al. a 1978, De Faria et al. a 1997]
323	4.6	FeIII-O	[Legodi, M.A., 2008]
375	4.85	Se-Se	[Manoharan, R. and Sethi, N., 2003, Edwards, H.G., 2005, Silverstein et al. 2014]
407	8.07	FeII-O	[Thibeau et al. 1978, De Faria et al. 1997]
464	4.31	Si-O-Si	[Manoharan, R. and Sethi, N., 2003, Edwards, H.G., 2005, Silverstein et al. 2014, Socrates, G., 2004]
491	4.36	FeII-O	[Thibeau et al. 1978, De Faria et al. 1997, Shebanova ON et al. 2003]
514	3.09	S-S	[Edwards,H.G.,2005, Shebanova ON et al. 2003, Manoharan, R. and Sethi, N., 2003]
610	7.3	FeII-O	[Hanesch M. 2009]
660	6.26	FeIII-O	[Oh et al. 1998]

685	7.8	C=S	[Thibeau et al. 1978, De Faria et al. 1997, [Shebanova ON et al. 2003]
713	14.1	FeIII-O	[Legodi, M.A., 2008]
764	5.0	C-F	[Edwards,H.G.,2005, Silverstein et al. 2014]
784	5.2	C-F	[Edwards, H.G., 2005, Silverstein et al. 2014]

Figure (4.2) shows the Raman spectrum of magnetite after irradiation with Nd-YAG laser. The spectrum shows clear peaks and by comparison with the vibrations recorded in some references we found that these vibrations are attributed to some components of materials that are listed in table (4.2).

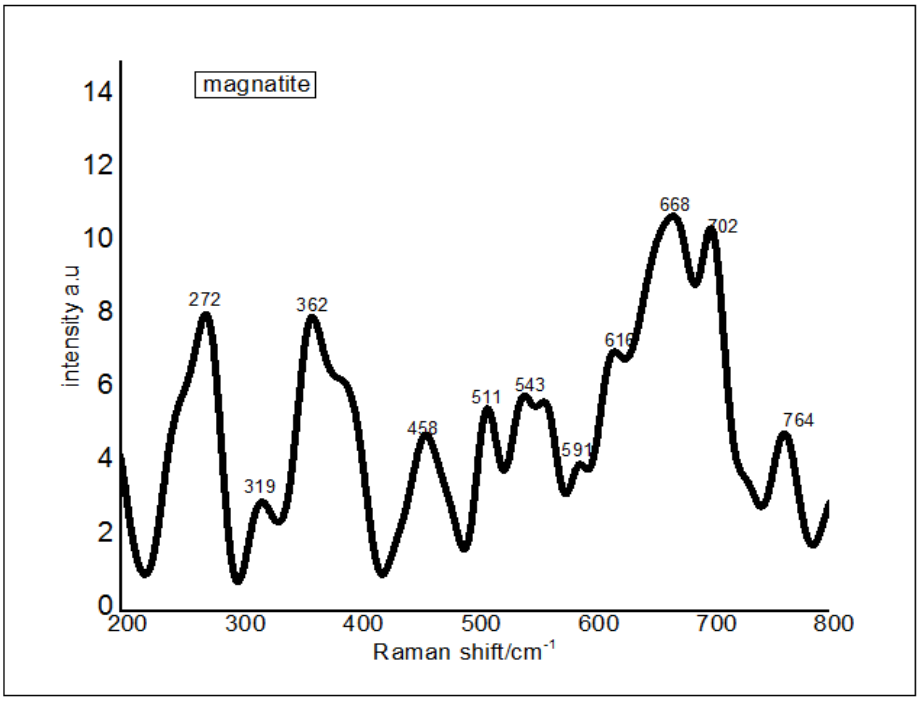

Fig (4.2): Raman spectrum of magnetite in the range (200 cm^{-1} to 800cm^{-1}).

Table (4.2): The analyzed data of Raman spectrum of the magnetite

Raman shift (cm^{-1})	Intensity (a.u)	Assignment	References
272	8.6	FeII-O	[Legodi, M.A. and De Waal, D., 2007, Kumar, C.S. ed., 2012]
319	4.3	FeIII-O	[Shebanova, O.N. and Lazor, P., 2003]
362	8.34	Se-Se	[Ferraro, J.R.,2003, Manoharan, R. and Sethi, N., 2003, Silverstein et al. 2014]
457	5.84	Si-O-Si	[Ferraro, J.R.,2003, Manoharan, R. and Sethi, N., 2003, Silverstein et al. 2014, Socrates, G., 2004]
511	6.61	S-S	[Ferraro, J.R., 2003 , Manoharan, R. and Sethi, N., 2003, Silverstein et al. 2014]
543	7.3	Fe III-O	[Hanesch M. 2009, Oh et al. 1998, Kumar, C.S. ed., 2012]
591	4.5	C=S	[Manoharan, R. and Sethi, N., 2003, Socrates, G., 2004]
616	8.4	FeIII-O	[Shebanova, O.N. and Lazor, P., 2003]
668	11.98	FeIII-O	[Hanesch M. 2009, Oh et al. 1998, Kumar, C.S. ed., 2012]
702	11.5	FeII-O	[Legodi, M.A. and De Waal, D., 2007]
764	5.31	C-F	[Manoharan, R. and Sethi, N., 2003, Socrates, G., 2004]

Figure (4.3) shows the Raman spectrum of goethite after irradiation with the doubled frequency Nd-YAG laser. The vibrations of goethite are appeared in the spectrum beside the vibrations of unstable components of goethite and other materials. These vibrations are consistent with many of previous studies as listed in table (4.3)

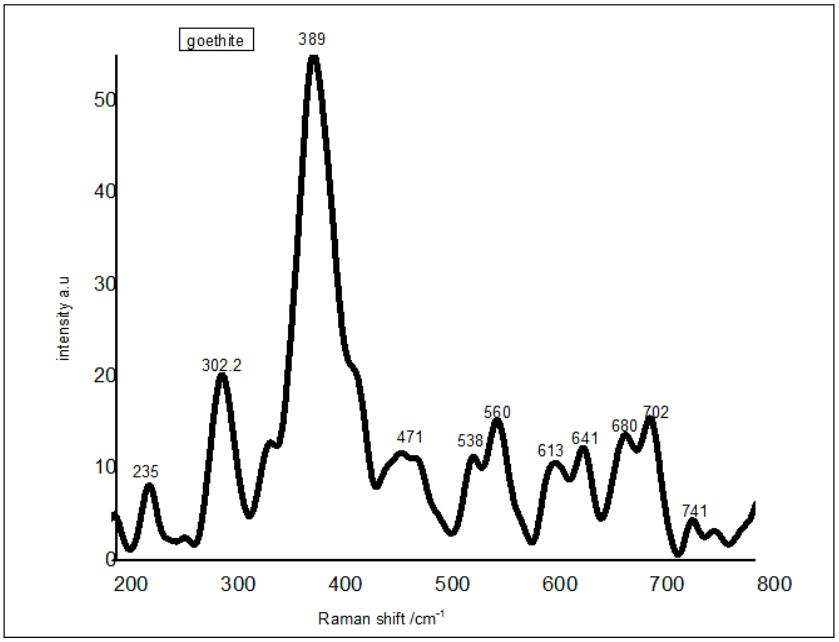

Figure (4.3): Raman spectrum of goethite in the range from 200 to 800 cm^{-1}

Table (4.3): The analyzed data of Raman spectrum of the goethite

Raman shift (cm^1)	Intensity (a.u)	Assignment	References
235	10.6	α Fe-OH	[De Faria et al. 1997, Oh et al. 1998]
302.2	23.4	α Fe-OH	[De Faria et al. 1997, Oh et al. 1998]
389	56	α Fe-OH	[De Faria et al. 1997, Oh et al. 1998]
471	14,8	α Fe-OH	[De Faria et al. 1997, Oh et al. 1998]
538	14.4	Si-O-Si	[Manoharan, R. and Sethi, N., 2003, Edwards, H.G., 2005, Silverstein et al. 2014, Socrates, G., 2004]
560	16.0	α Fe-OH	[De Faria et al. 1997, Oh et al. 1998]
613	13.7	FeII-O	[Thibeau et al. 1978]

641	15.3	C= S	[Manoharan, R. and Sethi, N., 2003, Edwards, H.G., 2005, Silverstein et al. 2014]
680	15.7	α Fe-OH	[Oh et al. 1998]
702	18.2	FeII-O	[Legodi, M.A. and De Waal, D., 2007]
741	6.8	C-F	[Edwards, H.G., 2005, Silverstein et al. 2014]

Figure (4.4) shows the Raman spectrum in the range from 200 to 800cm^{-1} of akaganeite. The vibrations of the akaganeite are appeared in the spectrum beside unstable components and some other materials. These results are in agreement with some previous studies as illustrated in table (4.4).

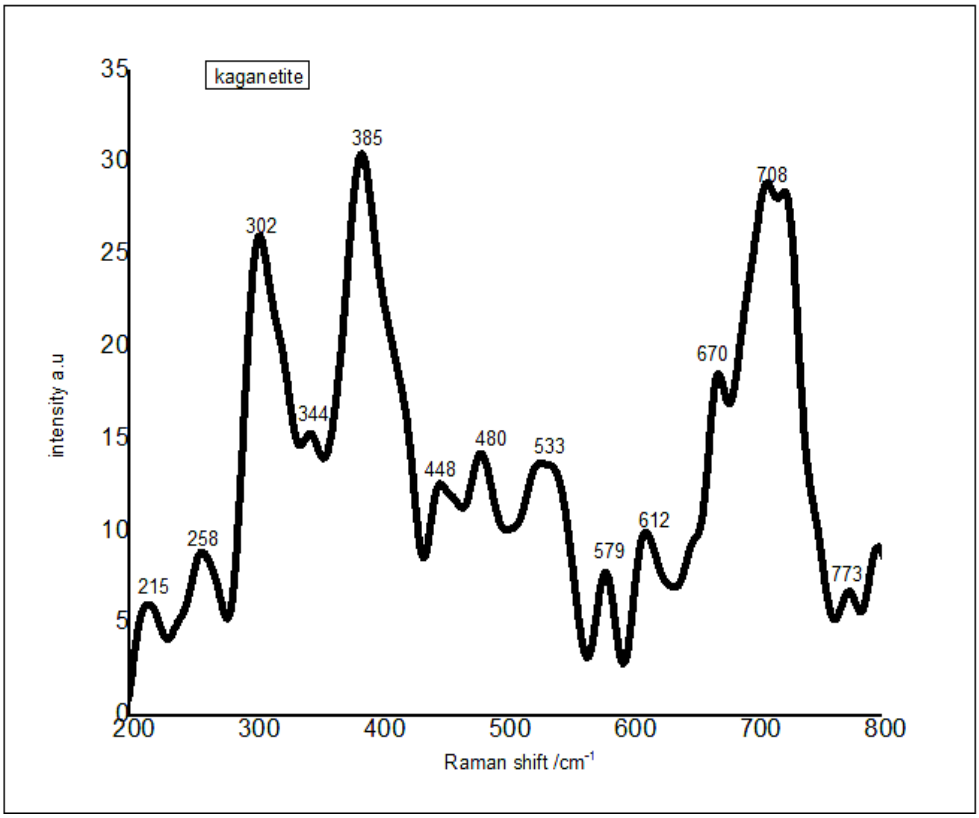

Figure (4.4): Raman spectrum of akaganeite in the range from 200 -800 cm^{-1}

Table (4.4): The analyzed data of Raman spectrum of the akaganeite

Raman shift (cm^1)	tensity (a.u)	Assignment	References
215	8.6	FeII-O	[De Faria et al. 1997, Thibeau et al. 1978]
258	11.3	FeII-O	[Thibeau et al. 1978]
302	26.3	β−FeOOH	[De Faria et al. 1997, Shebanova ON et al. 2003]
385	30.6	βFe-OH	[De Faria et al. 1997, Shebanova ON et al. 2003]
344	17.2	Se- Se	[Edwards, H.G., 2005, Manoharan, R. and Sethi, N., 2003, Silverstein et al. 2014, Socrates, G., 2004]
448	14	S-S	[Edwards, H.G., 2005, Manoharan, R. and Sethi, N., 2003, Silverstein et al. 2014, Socrates, G., 2004]
480	16.1	βFe-OH	[Shebanova, O.N. and Lazor, P., 2003]
533	16	βFe-OH	[Shebanova, O.N. and Lazor, P., 2003]
579	10.34	C= S	[Edwards, H.G., 2005, Silverstein et al. 2014, Manoharan, R. and Sethi, N., 2003]
612	11.15	βFe-OH	Shebanova, O.N. and Lazor, P., 2003
670	20.5	βFe-OH	[Shebanova, O.N. and Lazor, P., 2003]
708	29.3	βFe-OH	[De Faria et al. 1997, Shebanova, O.N. and Lazor, P., 2003]
773	8.31	C-F	[Edwards, H.G., 2005, Silverstein et al. 2014]

Figure (4.5) shows the Raman spectrum in the range from 200 ^{to} 800 cm^{-1} of 2-line ferrihydrite sample after irradiation with Nd-YAG laser with wavelength of 532 nm and 5mW power. This spectrum shows peaks of 2-line ferrihydrite molecules and some components of other materials that are listed in table (4.5)

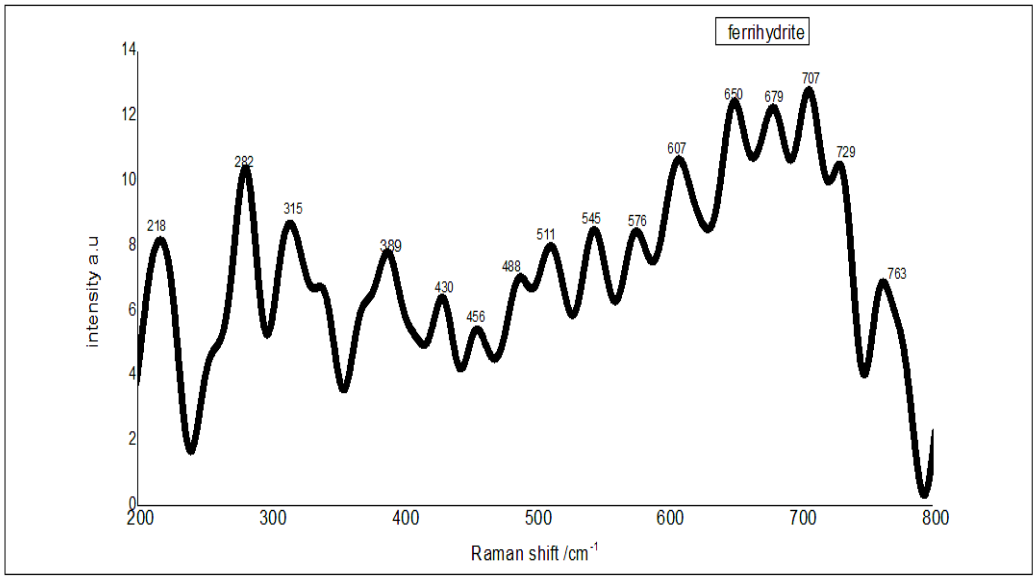

Figure (4.5): Raman spectra of ferrihydrite in the range from 200 cm^{-1} to 800cm^{-1}

Table (4.5): The analysis of Raman spectrum of 2-line ferrihydrite

Raman shift (cm^{-1})	Intensity (a.u)	Assignment	References
763	7.12	C-F	[Ferraro, J.R., 2003, Silverstein et al. 2014]
729	11.19	C-F	[Ferraro, J.R.,2003, Silverstein et al. 2014]
707	13.3	Fe-OH	[Hanesch M. 2009]
679	12.9	C=S	[Manoharan, R. and Sethi, N., 2003, Socrates, G., 2004]
650	13.0	FeII-O	[De Faria et al. 1997]
607	10.95	FeII-O	[De Faria et al. 1997, Kumar, C.S. ed., 2012]

576	8.7	C-Cl	Manoharan, R. and Sethi, N., 2003, Socrates, G., 2004]
545	9.09	Si -O- Si	[Manoharan, R. and Sethi, N., 2003, Socrates, G., 2004]
511	8.4	Fe-OH	[Hanesch M. 2009]
488	7.6	FeII-O	[Thibeau et al. 1978, Oh et al. 1998]
456	6.62	Si-O-Si	[Ferraro, J.R.,2003, , Manoharan, R. and Sethi, N., 2003, Silverstein et al. 2014, Socrates, G., 2004]
430	7.0	S- S	[Manoharan, R. and Sethi, N., 2003]
389	8.2	Fe-OH	[Hanesch M. 2009]
315	8.97	FeIII-O	[Oh et al. 1998]
282	10.9	FeII-O	[Oh et al. 1998, Thibeau et al. 1978]
218	8.6	FeII-O	[De Faria et al. 1997, Oh et al. 1998, Thibeau et al. 1978]

Through the analysis of the five samples results, it was found that the vibration modes of some materials are appeared as follows:

1- FeII-O appeared in the spectra of the five samples at different intensities (10.7, 8.51, 2.8, 8.07, 4.36, 7.3, 8.6, 11.5, 13.7, 18.2, 8.6, 11.3, 13, 10.95, 7.6, and 10.9).

2- FeIII-O appeared in the spectra of the hematite, magnetite and 2line ferrihydrite at different intensities (4.6, 6.26, 14.1, 4.3, 7.3, 8.4, 11.98, and 8.97).

3- αFe-OH appeared in the spectrum of the goethite with different intensities (10.6, 23.4, 56, 14.8, 16, and 15.7).
4- βFe-OH appeared in the spectrum of the akaganeite with different intensities (26.3, 30.6, 16.1, 16, 11.15, 20.5, and 29.3).
5- Fe-OH appeared in the spectrum of 2line ferrihydrite at different intensities (13.3, 8.4, and 8.2).
6- Si -O- Si appeared in the spectra of the hematite, magnetite, goethite and 2-line ferrihydrite samples with different intensities (4.31, 5.84, 14.4, and 6.62).
7- C= S appeared in the spectra of the five samples with the following Intensities, respectively. (7.8, 4.5, 15.3, 10.34, and 12.9).
8- Se-Se appeared in spectra of hematite, akaganeite and ferrihydrite with different intensities (4.85, 17.2, and 8.97).
9- S- S appeared in the spectra of the hematite, magnetite, akaganeite and ferrihydrite with different intensities (3.09, 6.61, 14, and 7.0).
10- C-Cl appeared in the spectrum of the ferrihydrite with intensity (8.7).
11- C-f appeared in the spectra of the five samples with different intensities (5.0, 5. 2, 5.31, 6.8, 8.31, 7.12and 11.19).

The bands that proved to be useful for the identification of the investigated hematite are listed in Tables (4-1). Six vibration modes of FeII-O at 288, 220, 407 $cm^{-1,}$ 491,610 and 252 cm^{-1} are agreed with the literature (Thibeau et al. 1978, De Faria et al. 1997) . Also the vibrational modes at 713 cm^{-1}, 660 cm^{-1} and 323 cm^{-1} were observed. These are assigned to Magnetite and this agreed with the results of other research (Shebanova, O.N. and Lazor, P., 2003). Vibration modes of other materials are observed at 464 cm^{-1} and assigned to silicate, 685 cm^{-1} assigned to alkyl sulfides, 514 cm^{-1} assigned to dialkyl disulfide, 774 cm^{-1} and 784 cm^{-1} which are assigned to Aliphatic fluoro according to [Edwards, H.G., 2005, Manoharan, R. and Sethi, N., 2003, Silverstein et al.2014 , Socrates, G., 2004].

Table (4-2) illustrate that most of the Raman shift for vibration modes of materials are located between 200 -800 cm^{-1}. Four vibrational modes of FeIII-O at 668 cm^{-1}, 543cm^{-1}, 616 cm^{-1} and 319 cm^{-1} are assigned to magnetite and mentioned in the literatures (Oh et al. 1998). Very high intensity of FeII-O vibration modes are appeared in the spectra at 272 cm^{-1} and 702 cm^{-1} and they assigned to hematite as mentioned in the literatures (Thibeau et al. 1978). Also other vibration modes of materials are appeared at 457 cm^{-1} and assigned to silicate, at 511 cm^{-1} assigned to dialkyl disulfide, 591cm^{-1} assigned to alkyl sulfides, and at 764 cm^{-1} assigned to Aliphatic Fluoro according to [Edwards, H.G., 2005, Manoharan, R. and Sethi, N., 2003, Silverstein et al.2014, Socrates, G., 2004].

In the Raman spectrum of Goethite there are vibrational modes of α Fe-OH with high intensity appeared at 389 $cm^{-1,}$ 235, 302.2, 389, 471, 560 and 681 cm^{-1} and are assigned to goethite as mentioned in the literatures (Oh et al. 1998). Also we found vibrations mode of FeII-O that appeared in the spectra at 702 and 613 cm^{-1} which assigned to hematite as mentioned in the literatures (Thibeau et al. a 1978, De Faria al. a 1997). Other materials vibration mode at 538 cm^{-1} and assigned to silicate, vibration mode at 641 cm^{-1} attributed to alkyl disulfide and mode at 741 assigned to aliphatic fluoro were noticed and this agreed with the results of other research's, [Edwards, H.G., 2005, Manoharan, R. and Sethi, N., 2003, Silverstein et al.2014, , Socrates, G., 2004].

For akaganeite seven vibration modes of βFe-OH appeared at 302, 385, 708 cm^{-1}, 490, 533, 612 and 670 cm^{-1} are assigned to akaganeite as presented in the literature (Oh et al.1998). In addition to FeII-O vibration modes, bands at 215 and 258 cm^{-1} are appeared which attributed to hematite according to (Thibeau et al. 1978, De Faria al. 1997). Other vibration modes for other materials were observed at 448 cm^{-1} and assigned to dialkyl disulfide, 579 cm^{-1} assigned to alkyl disulfide, 773 cm^{-1} assigned to aliphatic fluorin

according to [Edwards, H.G., 2005, Manoharan, R. and Sethi, N., 2003, Silverstein et al.2014, , Socrates, G., 2004].

For the peaks of 2-line ferrihydrite listed in table 4-5, three vibration modes of Fe-OH are appeared at 707 $cm^{-1,}$511 cm^{-1} and 389 cm^{-1} which assigned to ferrihydrite and this agreed with the results of other research (Hanesch M. 2009). Other peaks are appeared at 282 cm^{-1}, 650 cm^{-1}, 607 cm^{-1}, 218 and 488 cm^{-1} and assigned to hematite as mentioned by (De Faria et al. a 1997). The laser power of 5mW is sufficient to convert the ferrihydrite to hematite in addition to the appearance of vibration mode at 315 cm^{-1} attributed to magnetite according to (Oh et al. 1998). Other vibration modes were found at 458 cm^{-1} and assigned to silicate, 679 cm^{-1} assigned to alkyl sulfides, 430 cm^{-1} assigned to dialkyl disulfide, 576 cm^{-1} assigned to primary chlorolkanes and 763 cm^{-1} and 729 cm^{-1} which are assigned to Aliphatic fluorine (Ferraro, J.R., 2003, Manoharan, R. and Sethi, N., 2003,Silverstein et al.2014, , Socrates, G., 2004).

4.3: Conclusions

From the obtained results one can conclude that:

1. Laser Raman spectroscopy technique is easy, its results are obtained in a short period of time and little sample preparation is required for Raman experiments.

2. Laser Raman spectroscopy technique is an efficient method to identify the unstable compounds of hematite, magnetite, goethite, akaganeite and 2-line ferrihydrite.

3. Precise information about other materials can be obtained from the five samples.

4. Also Raman spectroscopy can distinguish between the hematite, magnetite, goethite, and akaganeite and 2line ferrihydrite efficiently.

4.4: Recommendations

The most important points recommended as future study are

1. Studying the effect of laser power on the Raman spectra of the same samples.
2. The study of unstable compounds in some medical samples.
3. Using Raman microscope for imaging and comparing the images with the spectra.
4. Measurement of Raman spectra starts with the lowest possible laser power to obtain high quality spectra (sharp bands) to avoid any destruction of sample.

References

Amer, M. ed., (2009). Raman spectroscopy for soft matter applications. John wiley & Sons .Canada.

Bakeev, K.A. ed., (2010). *Process analytical technology: spectroscopic tools and implementation strategies for the chemical and pharmaceutical industries*. John Wiley & Sons. USA.

Beaty, R.D. and Kerber, J.D., (1978). *Concepts, instrumentation and techniques in atomic absorption spectrophotometry* (p. 27). USA: Perkin-Elmer.

Besson, J.P., (2006). *Photoacoustic spectroscopy for multi-gas sensing using near infrared lasers* . Swiss.

Boss, C.B. and Fredeen, K.J., (1999). Concepts, instrumentation and techniques in inductively coupled plasma optical emission spectrometry. Norwalk: Perkin Elmer.

Bumbrah, G.S. and Sharma, R.M., (2016). Raman spectroscopy–Basic principle, instrumentation and selected applications for the characterization of drugs of abuse. *Egyptian Journal of Forensic Sciences*, *6*(3), pp.209-215.

Chatgilialoglu, C., Ferreri, C., Melchiorre, M., Sansone, A. and Torreggiani, A., (2013). Lipid geometrical isomerism: from chemistry to biology and diagnostics. *Chemical Reviews*, *114*(1), pp.255-284.

Cornell, R.M. and Schwertmann, U., (2003). *The iron oxides: structure, properties, reactions, occurrences and uses*. John Wiley & Sons. Germany.

Cremers, D.A. and Knight, A.K., (2006). *Laser Induced Breakdown Spectroscopy*. John Wiley & Sons, Ltd. England.

De Faria, D.L.A., Venâncio Silva, S. and De Oliveira, M.T., (1997) . Raman microspectroscopy of some iron oxides and oxyhydroxides. *Journal of Raman spectroscopy*, *28*(11), pp.873-878.

Berman, P.R. and Malinovsky, V.S.,(2010). Principles of laser spectroscopy and quantum optics. Princeton University Press.

Demtröder, W., (2013). Laser spectroscopy: basic concepts and instrumentation. Springer Science & Business Media.

Dent, G. and Smith, G., (2005). *Modern Raman spectroscopy: a practical approach*. Wiley. England.

Ding, J., (2010). *The pH determination of palaeofluids: experimental and thermodynamic approach* .Nanjing University.

DR.H.Kaur .,(2001). "spectroscopy" first additions .

Edwards, H.G., (2005). Modern Raman spectroscopy—a practical approach. Ewen Smith and Geoffrey Dent. John Wiley and Sons Ltd, Chichester, 2005. Pp. 210. ISBN 0 471 49668 5 (cloth, hb); 0 471 49794 0 (pbk).

Esmonde-White, K.A., 2009. *Raman spectroscopy detection of molecular changes associated with osteoarthritis*, (Michigan).

Ferraro, J.R., (2003). *Introductory Raman spectroscopy*. Academic press.

García, R. and Báez, A.P., (2012). Atomic absorption spectrometry (AAS). In *Atomic Absorption Spectroscopy*. InTech.

Gardiner, D.J., (1989). Introduction to Raman scattering. In *Practical Raman Spectroscopy* (pp. 1-12). Springer Berlin Heidelberg.

Gilson, T.R. and Hendra, P.J., (1970). Laser Raman spectroscopy: a survey of interest primarily to chemists, and containing a comprehensive discussion of experiments on crystals. John Wiley & Sons.

Gustafsson, U., (1993). Near-infrared Raman Spectroscopy using Diode Laser and CCD Detector for Tissue Diagnostics. *Lund Reports in Atomic Physics*.

Hanesch, M., (2009). Raman spectroscopy of iron oxides and (oxy) hydroxides at low laser power and possible applications in environmental magnetic studies. *Geophysical Journal International*, *177*(3), pp.941-948. *Austria.*

Hassan, S.S., El Azab, W.I., Ali, H.R. and Mansour, M.S., (2015). Green synthesis and characterization of ZnO nanoparticles for photocatalytic

degradation of anthracene. *Advances in Natural Sciences: Nanoscience and Nanotechnology*, *6*(4), p.045012

Hassanein, R., (2011). *Rapid and Direct Food Investigation Using Raman Spectroscopy* . Jacobs University Bremen.

Ivković, R., Petrović, M., Jakšić, B., Cerić, V. and Milošević, M., 2016. Digital Image fundaments through Visible Spectrum. (Serbia).

Joshi, M., Bhattacharyya, A. and Ali, S.W., (2008). Characterization techniques for nanotechnology applications in textiles. India.

Kiefer, J., (2015). Recent advances in the characterization of gaseous and liquid fuels by vibrational spectroscopy. *Energies*, *8*(4), pp.3165-3197, Switzerland.

Kumar, C.S. ed., (2012). *Raman spectroscopy for nanomaterials characterization*. Springer Science & Business Media.Berlin Heidelberg.

Kumar, S., 2006. Spectroscopy of organic compounds. *Cosmic rays*, *10*, p.4.

Kumar, S., Kumar, V. and Jain, D.C., (2013). Laser Raman Spectroscopic Studies on Hemeproteins in Epileptic Children. *Open Journal of Applied Sciences*, *3*(01), p.123. India

Le Ru, E. and Etchegoin, P., (2008). *Principles of Surface-Enhanced Raman Spectroscopy: and related plasmonic effects* . *Victoria University of Wellington.*

Legodi, M.A. and De Waal, D., (2007). The preparation of magnetite, goethite, hematite and maghemite of pigment quality from mill scale iron waste. *Dyes and Pigments*, *74*(1), pp.161-168 .South Africa.

Legodi, M.A., (2008). *Raman spectroscopy applied to iron oxide pigments from waste materials and earthenware archaeological objects* .Pretoria.

Solarz, R.W. and Paisner, J.A., (1986). *Laser spectroscopy and its applications* (Vol. 11). CRC Press.

Lewis, I.R. and Edwards, H., (2001). *Handbook of Raman spectroscopy: from the research laboratory to the process line*. CRC Press.

Li, C. and Wu, Z., (2003). *Microporous materials characterized by vibrational spectroscopies* (pp. 423-513). Marcel Dekker Inc.: New York.

Lin, J.M. and Yamada, M., (2003). Microheterogeneous systems of micelles and microemulsions as reaction media in chemiluminescent analysis. *TrAC Trends in Analytical Chemistry*, *22*(2), pp.99-107.

Lin-Vien, D., Colthup, N.B., Fateley, W.G. and Grasselli, J.G., 1991. The handbook of infrared and Raman characteristic frequencies of organic molecules. New York.

Long, D.A., (2002). Quantum Mechanical Theory of Rayleigh and Raman Scattering. *The Raman Effect: A Unified Treatment of the Theory of Raman Scattering by Molecules*, pp.49-84.

Lopes, J.A., (2005). Process analytical technology: spectroscopic tools and implementation strategies for the chemical and pharmaceutical industries. Katherine A. Bakeev, Blackwell Publishing Ltd., Oxford, (2005), 451 pp, ISBN 1-4051-2103-3. *Journal of Chemometrics*, *19*(11-12), pp.668-669.

Lu, J.F. and Tsai, C.J., 2014. Hydrothermal phase transformation of hematite to magnetite. *Nanoscale research letters*, *9*(1), pp.1-8 .Taiwan.

Manoharan, R. and Sethi, N., 2003. 8.51 Raman Analyzers.

McCreery, R.L., (2005). *Raman spectroscopy for chemical analysis* (Vol. 225). John Wiley & Sons. New York, USA .

Nafie A. Almuslet., (2009). Lasers in Spectroscopy. Purchasing nova PDF

Naglic, P., 2012. Raman spectroscopy for medical diagnostics. *University of Ljubljana*

Oh, S.J., Cook, D.C. and Townsend, H.E., (1998). Characterization of iron oxides commonly formed as corrosion products on steel. *Hyperfine interactions*, *112*(1-4), pp.59-66. USA.

Reichenbächer, M. and Popp, J., (2012). *Challenges in molecular structure determination*. Springer Science & Business Media.Berlin Heidelberg.

Robertson, I., (2000). *Applications of Raman spectroscopy and chemometrics to semiconductor process control* (Dublin City University).

Sanchez-Rodas, D., Corns, W.T., Chen, B. and Stockwell, P.B., 2010. Atomic fluorescence spectrometry: a suitable detection technique in speciation studies for arsenic, selenium, antimony and mercury. *Journal of Analytical Atomic Spectrometry*, *25*(7), pp.933-946.

Sasic, S. ed., (2008). *Pharmaceutical applications of Raman spectroscopy*. John Wiley & Sons.Canada.

Schmidt, F., (2007). *Laser-based absorption spectrometry,(* Umea, Sweden)

Schwertmann, U. and Cornell, R.M., 2008. *Iron oxides in the laboratory: preparation and characterization*. John Wiley & Sons. .Germany.

Shebanova, O.N. and Lazor, P., (2003). Raman spectroscopic study of magnetite (FeFe 2 O 4): a new assignment for the vibrational spectrum. *Journal of Solid State Chemistry*, *174*(2), pp.424-430.

Silverstein, R.M., Webster, F.X., Kiemle, D.J. and Bryce, D.L., 2014. *Spectrometric identification of organic compounds*. John wiley & sons. New York.

Smith, E. and Dent, G., (2005). Introduction, basic theory and principles. *Modern Raman spectroscopy-A practical approach*, pp.1-21. England.

Socrates, G., (2004). *Infrared and Raman characteristic group frequencies: tables and charts*. John Wiley & Sons. New York

Solé, J., Bausa, L. and Jaque, D., (2005). *An introduction to the optical spectroscopy of inorganic solids*. John Wiley & Sons. England .

.

Straughan, B. ed., (2012). *Spectroscopy: Volume Three*. Springer Science & Business Media.

Stuart, B.H., (2004). Biological applications. *Infrared spectroscopy: fundamentals and applications*, pp.137-165.

Sur, U.K., (2013). Surface-enhanced Raman scattering (SERS) spectroscopy: a versatile tool in electrochemistry. *Research & Reviews in Electrochemistry*, *4*(3).

Taher, A.A.M., (2014). *Exploration of Singlet Oxygen Emitted After Irradiation of Dibenzocyanine 45, MethyleneBlue and Rhodamine 6G Dyes Using Lasers with Different Wavelengths* .Sudan University of Science & Technology, Sudan.

Thibeau, R.J., Brown, C.W. and Heidersbach, R.H., (1978). Raman spectra of possible corrosion products of iron. *Applied Spectroscopy*, *32*(6), pp.532-535.

Tu, A.T., (1982). *Raman spectroscopy in biology: principles and applications*. John Wiley & Sons .USA..

Vašková, H., (2011). A powerful tool for material identification: Raman spectroscopy. *Int. J. Math. Appl. Math.* Modell, *5*(7), pp.1205-1212

Wang, P., Sawatzki, J. and Tague, T.J., (2016). Innovative Applications of Raman Microscopy. *Microscopy and Microanalysis*, *22*(S3), pp.374-375.